Journal of Contaminant Hydrology 274 (2025) 104659

Contents lists available at ScienceDirect

Journal of Contaminant Hydrology

journal homepage: www.elsevier.com/locate/jconhyd

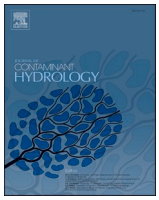

# Dynamics of potentially toxic elements in small rivers during high-flow events

Steffen Kittlaus [a,*], Radmila Milačič Ščančar [b,c], Katarina Kozlica [b], Nikolaus Weber [a], Jörg Krampe [a], Matthias Zessner [a], Ottavia Zoboli [a]

[a] TU Wien, Institute for water quality and resource management, Karlsplatz 13/E226-1, 1040 Vienna, Austria
[b] Jožef Stefan Institute, Department of Environmental Sciences, Jamova 39, 1000 Ljubljana, Slovenia
[c] Jožef Stefan International Postgraduate School, Jamova 39, 1000 Ljubljana, Slovenia

ARTICLE INFO

*Keywords:*
Water pollution
Discharge event
Concentration dynamics
Soil
Sediment
Suspended particulate matter (SPM)

ABSTRACT

This study investigates the concentration dynamics of potentially toxic elements (PTE) during flow events to improve process understanding of the transport dynamics and derive conclusions for monitoring and management.

The case study is a medium-sized lowland river catchment (387 km$^2$) with mainly agricultural and urban land use. Three-to-four events were sampled at three monitoring sites in sub-catchments with different characteristics, with one-to-six samples taken per event. Total and dissolved concentrations of 29 major and trace elements were analysed, and concentrations in suspended particulate matter (SPM) derived by calculation. This was complemented by 10 riverbed sediment sample and 10 soil composite samples collected through a land-use stratified sampling design, ensuring high representativeness of soil across the entire catchment.

The results confirm that PTE transport is primarily driven by the transport of SPM, but the PTE content in SPM exhibits distinct and systematic dynamics. Higher content of road traffic related elements (e.g. Sb) at earlier stages of the event indicates street runoff inputs, which has important implications for selecting effective emissions mitigation measures. Variability in both SPM transport and its quality has major implications for designing fit-for-purpose monitoring, for example for the accurate estimation of river loads or at the identification of contamination sources.

The investigation of the dissolved fraction of the PTE concentrations shows significant differences between some events and therefore offers high potential to discriminate between different event types. Furthermore, we were able to identify the duration of the pre-event low-flow period as a possible driver for differences in events. The contamination level found in the catchment is low to moderate, with no exceedance of environmental quality standards.

The calculation of enrichment factors identifies elements impacted by anthropogenic emissions, indicating important pollution sources and pathways. This is key to effective management.

## 1. Introduction

River pollution by heavy metals or more broadly potentially toxic elements (PTE) is an important issue in many waterbodies worldwide (Li et al., 2020; Saravanan et al., 2024). The term "potentially toxic elements" was introduced to summarize elements that are toxic if they occur in the environment at elevated concentrations. What compounds are captured under this term varies, often encompassing metals (V, Cr, Mo, Mn, Fe, Co, Ni, Cu, Zn, Cd, Hg, Al, Pb), some metalloids (As, Sb) and sometimes also certain non-metals (Se, Ba) (Pourret and Hursthouse, 2019). A thorough understanding of the emission sources and pathways, the transport and the impact of such elements on ecosystems is essential to implement appropriate monitoring programmes and identify and select effective and cost-efficient mitigation measures.

For many of these elements, the major share of the total load is transported during discharge events within the suspended particulate matter (SPM) load (Ciszewski and Grygar, 2016; Durrieu et al., 2023; Roussiez et al., 2013). Some studies even suggest to use SPM

* Corresponding author.
*E-mail address:* steffen.kittlaus@tuwien.ac.at (S. Kittlaus).

https://doi.org/10.1016/j.jconhyd.2025.104659
Received 20 March 2025; Received in revised form 24 June 2025; Accepted 25 June 2025
Available online 26 June 2025

concentration as proxy parameter for PTE as they found strong linear regression (Nasrabadi et al., 2018; Nasrabadi et al., 2016). However, there is limited knowledge about differences in contaminant transport between different catchments (Pulley et al., 2016) and the dynamics of contaminant concentrations within events (Barber et al., 2017).

Numerous studies have examined variations in PTE concentrations in rivers of different sizes and catchment characteristics under various flow conditions. Here, we briefly summarize the existing knowledge based on studies conducted in catchments with comparable characteristics and with a similar focus to this work.

In their review of flood-related storage and remobilization processes in polluted river systems Ciszewski and Grygar (2016) confirm the general positive relationship between suspended matter and heavy metal concentrations with river discharge. In some cases, the metal concentration remains high during flood attenuation, producing an anticlockwise hysteresis loop of metal load versus discharge and indicating the reactivation of temporary sinks of polluted sediments in the river system. For the dissolved concentrations, Ciszewski and Grygar (2016) found rising As content with rising flow, while for most metals, which are primarily transported in particulate form, the dilution effect resulted in decreasing dissolved concentrations with increasing flow. Most of these findings are confirmed by Milačič et al. (2017) in their comparison of PTE concentrations in the Sava River during a heavy high-flow event and under low-flow conditions. Milačič et al. (2017) do not confirm the exception for dissolved As concentrations, which they also found higher in low-flow samples compared to high-flow samples. The reason could be, that due to the huge magnitude of the high-flow event studied in the Sava River, even increased emissions of dissolved As during the event are eventually diluted by the huge amounts of water.

The dynamics of trace metals during rain events in two rivers heavily influenced by the urban area of Marseille (France) were investigated by Oursel et al. (2014) and found to be dependent on the river, the event and the investigated element for dissolved and total concentrations. Metal contamination was mainly driven by particulate transport in solids from urban impervious areas and soil erosion.

Trace element partitioning and enrichment was also investigated in a small urban river catchment (60 $km^2$) in the Mediterranean region by Durrieu et al. (2023) by sampling during one strong event and at base-flow conditions. The authors found that As, Cu, Co, Zn, Cd and Ni were mainly transported in dissolved form during base flow, while Pb was mainly transported in particulate form. During the flood event, all metals were mainly transported in particulate form, only As was still mainly in dissolved phase. When looking at the metal content in SPM during the flood event compared to low-flow conditions, the differences were small (0.4–2.5-fold) but significant: While a decrease in Cu and Cd was observed during the flood event, the content of Cr, Co, Ni, As, Zn and Al increased.

Temporal variations of metal enrichment in SPM was investigated in a rural catchment in Japan by Matsunaga et al. (2014). The two sampled events in a mainly forested catchment showed a negative correlation between metal content in SPM and discharge volume, which was explained by dilution of more contaminated particles from carbon enriched topsoil with less polluted lithological material from deeper sediment layers and bank material. This interpretation was supported by mineralogical analysis and carbon content analysis. The study also found that change in metal loading of SPM implies a change of metal partitioning between particulate and dissolved phase during different flow stages of events.

Metal (Al, Fe, Mn, Cu, Zn) concentrations dynamics during three rain events in a small (65 $km^2$) agricultural catchment in Spain were investigated by Palleiro et al. (2012). They found anticlockwise hysteresis for total metal concentrations against flow and dissolved metal concentration peaks after flow peak. They concluded that the metal source is far from the river and that subsurface transport of dissolved metals plays a role, without this being clearly justified.

Three flash-flood events in a small agricultural catchment (32.8 $km^2$) were sampled by Roussiez et al. (2013) in France. They observed clockwise hysteresis for dissolved metals during a strong event, no significant correlation between SPM concentrations and metal content (Al, Fe, Mn, Sc, Cr, Ni, Cu, Zn, Pb, As, Cd) in SPM but positive correlations between dissolved metal (Cr, As, Cu, Ni, Cd, Pb) concentration and discharge. The authors interpreted this as a contribution from the flushing of easily dissolvable material from topsoil layers accumulated during dry periods before the event, and metals desorbing from such particles during the event.

Effects of a large flooding event on water quality in rivers but also in wastewater and tap water was investigated by Barber et al. (2017). They found dilution effects of dissolved elements in headwaters, mobilisation of soluble elements from the landscape, including urban areas, and mobilisation of elements from the vadose zone by elevated groundwater levels and recharge.

The above-mentioned studies provide valuable insights into the dynamics of trace metals during flow events, but the knowledge base is still too limited to derive some general conclusions applicable to a wider range of catchments and flow events. Our study aims to contribute to broaden the knowledge base by investigating the dynamics of trace metals river transport in a medium size catchment (387 $km^2$) with 3 monitoring sites for a series of events of limited magnitude. Specifically, we address the following research questions:

a) Is the transport of trace metals during events mainly determined by the transport of SPM or does the metal content in the SPM change during the events? This has important implications for the requirements for monitoring during such events to determine metal loads: if the quality of SPM remains unchanged during the events, it would be sufficient to analyse only a few samples for their metal composition and combine this information with the SPM load, which in turn can be estimated with the help of inline monitoring with turbidity probes. Conversely, if the SPM composition changes significantly during events, either high frequency grab sampling or flow proportional integrated sampling over the entire event period would be necessary to properly determine metal loads.
b) If there is a dynamic of SPM composition during events, is the SPM more polluted at the beginning of the event? This may be indicative of urban pollution sources, where a very fast flushing of heavily polluted particles into the river is to be expected. This carries implications for the implementation of pollutant mitigation measures. For instance, stormwater runoff retention basins and soil filters can be used to catch such first flush contamination (Birch et al., 2006; Cederkvist et al., 2016).
c) Is there a systematic enrichment of metals during the process or soil erosion and sediment delivery? Such enrichment, caused be particle size shift, is reported for nutrients and some heavy metals (Fuchs and Schwarz, 2007; Quinton and Catt, 2007) and enrichment factors are applied in soil erosion emission modelling (Acosta Porras et al., 2016; Aksoy and Kavvas, 2005; Jiang et al., 2022; Venohr et al., 2011). This aspect of the study can therefore contribute to updating and revising existing enrichment factors and to deriving new ones.
d) Can the elemental composition of the SPM in the samples be used to determine the source of the sediment in the catchment? This would be beneficial to identify the main sediment sources in catchments.
e) What is the behaviour of the dissolved concentrations during events? While they are of minor importance for the transported trace metal loads during events, they are key for the aquatic toxicity for the ecosystem. In this respect, we also investigate whether critical levels are reached, which violate the environmental quality standards.
f) Are there significant differences in the composition of samples from different flow events and can these be attributed to specific driving factors?

An added value of this study is that we analysed the transport of PTE in the Wulka River (Austria), which is the main tributary of the Lake

Neusiedl. Lake Neusiedl is a flat, sub saline steppe lake (Hammer, 1986) without a natural outlet. This specific situation may lead to the accumulation and enrichment of persistent and mobile pollutants in the lake (Zessner et al., 2019; Zoboli et al., 2023), potentially endangering the health of this unique ecosystem. A better understanding of the inputs to the lake is therefore of utmost importance.

## 2. Material and methods

### 2.1. Study area

The Wulka (Fig. 1) is a lowland river in eastern Austria and the main tributary of Lake Neusiedl (Soja et al., 2013). As shown in Table 1, the catchment receives on average 669 mm of precipitation per year and has a potential evapotranspiration rate of about 888 mm per year (1991–2020), resulting in relatively dry conditions. Combined with the high input of treated wastewater in some of the sub catchments, and significant agricultural land use, the Wulka is a very interesting case study.

Samples were taken from two tributaries of the Wulka River and from the Wulka River itself after the confluence of the two tributaries. The tributaries have very different characteristics. The catchment of the Eisbach includes a large town and the effluent of its wastewater treatment plant (WWTP, ~28,000 population equivalents (p.e.), EMREG, 2024) contributes the majority of the river dry weather flow. The Nodbach has a similar catchment size area to the Eisbach but has no known wastewater inputs during dry weather and therefore has a much lower dry weather flow. The catchment of the Wulka River itself upstream of the sampling site, can be described as heavily influenced by human activities, both in the form of agriculture, with much viticulture, and settlements and their WWTP effluents. The second WWTP in the catchment has an incoming load of 70,736 p.e. (EMREG, 2024) and together with the WWTP in the Eisbach catchment this results in an average percentage of treated wastewater of 39 % of the total river flow in the Wulka.

### 2.2. Sampling

To study the dynamics of trace elements during high-flow events, 50 samples were collected from three rivers for 3–4 events each. These river event flow samples were supplemented with 10 bed sediment and 10 soil samples from the catchment to investigate relationships between catchment sediment sources and event samples.

#### 2.2.1. River event-flow sampling

Sampling of event flow took place between July 2021 and November 2022. These two years were moderately (2021) and extremely dry (2022) in the Wulka catchment, as indicated by the Standardized Precipitation Evapotranspiration Index (SPEI365) reported in Table 1 and classified according to Hayes (2005).

During events, triggered by an elevated water level, a series of 1 L water samples were taken with an automatic sampler (Endress+Hauser Liquistation CSF48) in a time-proportional manner. The equal time step of the sampling (50 min for Eisbach and Nodbach, 60 min for Wulka) was adapted to be able to cover the expected maximum event duration with the available 24 bottles. Within 3 days after the end of the events, the samples were collected from the cooled samplers and were transported to the laboratory in cold conditions. A subset of all samples was selected for further analysis. Recordings of water level and total suspended solids (TSS) concentration (modelled from turbidity measurement) from in-line sensors were plotted together with the sampling times, and samples for further analysis were selected to cover different stages of the events as well as possible (cp. Fig. 2).

A portion of each water sample was filtered immediately after

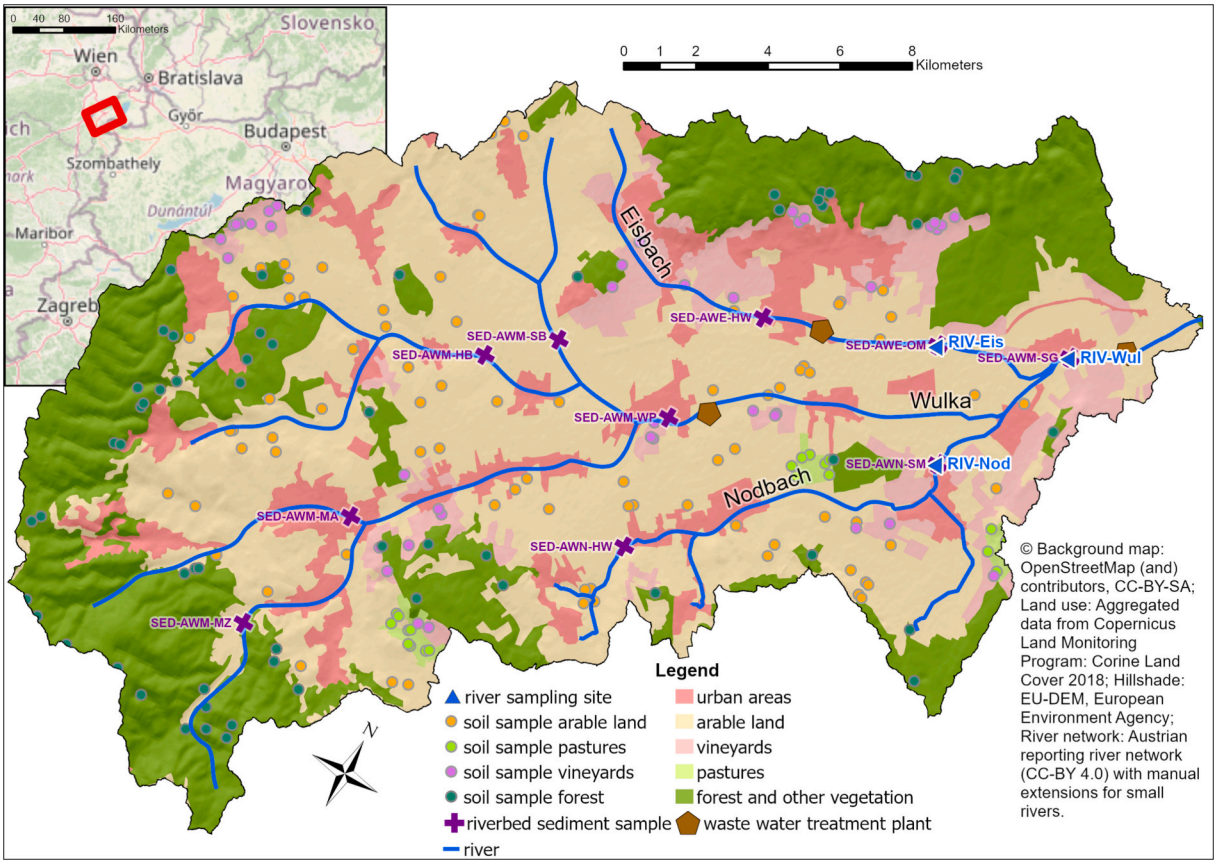


**Fig. 1.** Map of the Wulka catchment showing land use and sampling locations for water, sediment and soil.

**Table 1**
catchment properties of the three rivers studied.

| River | Wulka | Nodbach | Eisbach | Data source |
|---|---|---|---|---|
| Catchment area (km$^2$) | 387 | 64 | 65 | |
| Land use, cover and topography: | | | | Corine Land Cover 2018 (EEA, 2020a) |
| Arable land (%) | 44 | 54 | 33 | |
| Vineyards (%) | 8 | 6 | 18 | |
| Pastures (%) | 1 | 2 | 0 | |
| Forests and natural vegetation (%) | 28 | 21 | 30 | |
| Urban areas (%) | 13 | 11 | 18 | |
| Other land use (%) | 6 | 6 | 1 | |
| Impervious area (%) | 5.0 | 4.3 | 7.9 | Copernicus HRL Imperviousness 2018, 10 m (EEA, 2020b) |
| Mean altitude above sea level (m) | 261 | 201 | 229 | EU-DEM (EEA, 2016) |
| Climate & hydrology | | | | |
| mean annual temperature 1991–2020 (°C) | 10.9 | 11.3 | 11.1 | SPARTACUS v2.1 (Hiebl and Frei, 2016) |
| mean annual temperature 2021/2022 (°C) | 11.1/12.1 | 11.5/12.4 | 11.4/12.4 | |
| mean annual potential evapotranspiration 1991–2020 (mm/a) | 888 | 913 | 889 | WINFORE v2.1 2021/22 (Haslinger and Bartsch, 2016) |
| mean annual potential evapotranspiration 2021/22 (mm/a) | 910/957 | 938/986 | 912/960 | |
| mean annual precipitation 1991–2020 (mm/a) | 669 | 635 | 658 | SPARTACUS v2.1 (Hiebl and Frei, 2018) |
| annual precipitation 2021/22 (mm/a) | 529/452 | 510/410 | 525/420 | |
| Standardized Precipitation Evapotranspiration Index (SPEI365) 2021/22 (−) | −1.4/ −2.4 | −1.3/ −2.6 | −1.3/ −2.6 | WINFORE v2.1 2021/22 (Haslinger and Bartsch, 2016) |
| mean annual flow (m$^3$/s) | 1.12 | 0.09 | 0.19 | (Hydrographischer Dienst Burgenland, 2022) |
| specific runoff (mm/a) | 96 | 44 | 92 | |
| mean annual sediment load (t/km$^2$/a) | 2.3 | 0.7 | 2.1 | (Weber et al., 2025) |
| Anthropogenic pressure | | | | |
| total inhabitants (2021) (inh.) | 66,818 | 9308 | 19,693 | (EUROSTAT Gisco, 2023) |
| population density (inh./km$^2$) | 173 | 146 | 303 | (EUROSTAT Gisco, 2023) |
| percentage of treated municipal wastewater in mean annual river flow at the catchment outlet (%) | 39 | 0 | 50 | (EMREG, 2024) |

sample collection to investigate the dissolved fraction, and both total and filtered samples were acidified to avoid sorption to the bottles during storage.

All sampled events peaked significantly below mean annual high-flow (HQ1) discharge but above the mean annual flow (MQ) of the river (Fig. 2). All but one sample were taken at flow conditions above MQ. The only exception is sample “RIV-WUL-4-1”, which was taken from a discharge-wise very small event where the TSS peak occurred significantly after the discharge peak and flow was already below MQ at sampling time. As this event was below the water level trigger value, it was only sampled by chance (maintenance work at the station) and therefore only one sample is available from this event. As the inline measured TSS concentration of this event was the highest observed of all sampled events, it was decided to include it in the study, even though the event was not fully covered.

#### 2.2.2. River low-flow composite sampling

For comparison with the event flow samples, base flow conditions were sampled with a composite sampling approach: Weekly grab samples were combined into composite samples for the duration of two months (6–8 grab samples per composite depending on occurrence of high-flow). Samples were kept frozen until analysis. For further details see Kardos et al. (2024) and Milačič et al. (2023).

#### 2.2.3. Sediment sampling

Riverbed sediments were sampled with a polycarbonate corer at 10 sites distributed over the whole catchment (cp. Fig. 1). The upper 5–10 cm of sediment were sampled and 3–5 sub-samples per site were combined into one sample.

#### 2.2.4. Soil composite sampling

Soil samples were collected as spatial composite samples with land-use stratification. For each composite sample (4 from arable land, 2 from vineyards, 1 from pasture and 3 from forest), 20 sub-samples from different locations in the catchment (cp. Fig. 1) with the same land use were combined. On arable land and vineyards, the samples were collected from the upper 30 cm of the soil, while on pastures and in forests only the upper 10 cm were sampled.

### 2.3. Chemical analysis

The collected river water samples as well as the soil and sediment samples were analysed for 29 major and trace elements and additional supporting parameters like suspended solids and nutrients (N and P). The large number of parameters were analysed to retrieve additional information about the samples and therefore improve the chance to be able to detect patterns in the samples.

Even though there is some justified criticism of the term “potentially toxic elements” (Zhang et al., 2022) we use it in this manuscript to differentiate a wider general group of trace elements from those, which occur more frequently as water pollutants. In our analysis, we will use ”PTE” to refer to the most critical metals and metalloids (Cr, Ni, Cu, Zn, Cd, Pb, As, Sb) except from Hg, which we were not able to analyse.

#### 2.3.1. Determination of element and TSS concentrations in river water

To determine total concentrations of elements in river water, 3 mL of nitric acid, 0.1 mL of hydrofluoric acid and 1 mL of hydrochloric acid were added to 10 mL of sample and contents was subjected to microwave assisted digestion. After digestion, samples were 10-times diluted before analysis of element concentrations by inductively coupled plasma mass spectrometry (ICP-MS).

Dissolved concentrations of elements in river water samples were determined directly from the filtered and acidified samples by ICP-MS. All the analyses were performed in triplicate. Li, K, Rb, Ba, Sc, Y, La, Ce, Ti, Zr, V, Nb, Cr, Mn, Fe, Co, Ni, Cu, Ag, Zn, Cd, Al, Ga, Tl, Pb, As, Sb, Bi and Se were analysed by ICP-MS and the analytical limits as well as the detection frequency are reported in Table S1 in the Supplemental Material.

Low-flow composite samples were analysed in the same laboratory but derived within a different project (Kardos et al., 2024) and thus only PTE but no further elements were analysed in these samples.

Total suspended solids (TSS), N and P concentrations were analysed separately: TSS was analysed by filtration and gravimetry according to DIN 38409-2:1987-03, N by oxidative digestion with peroxodisulfate

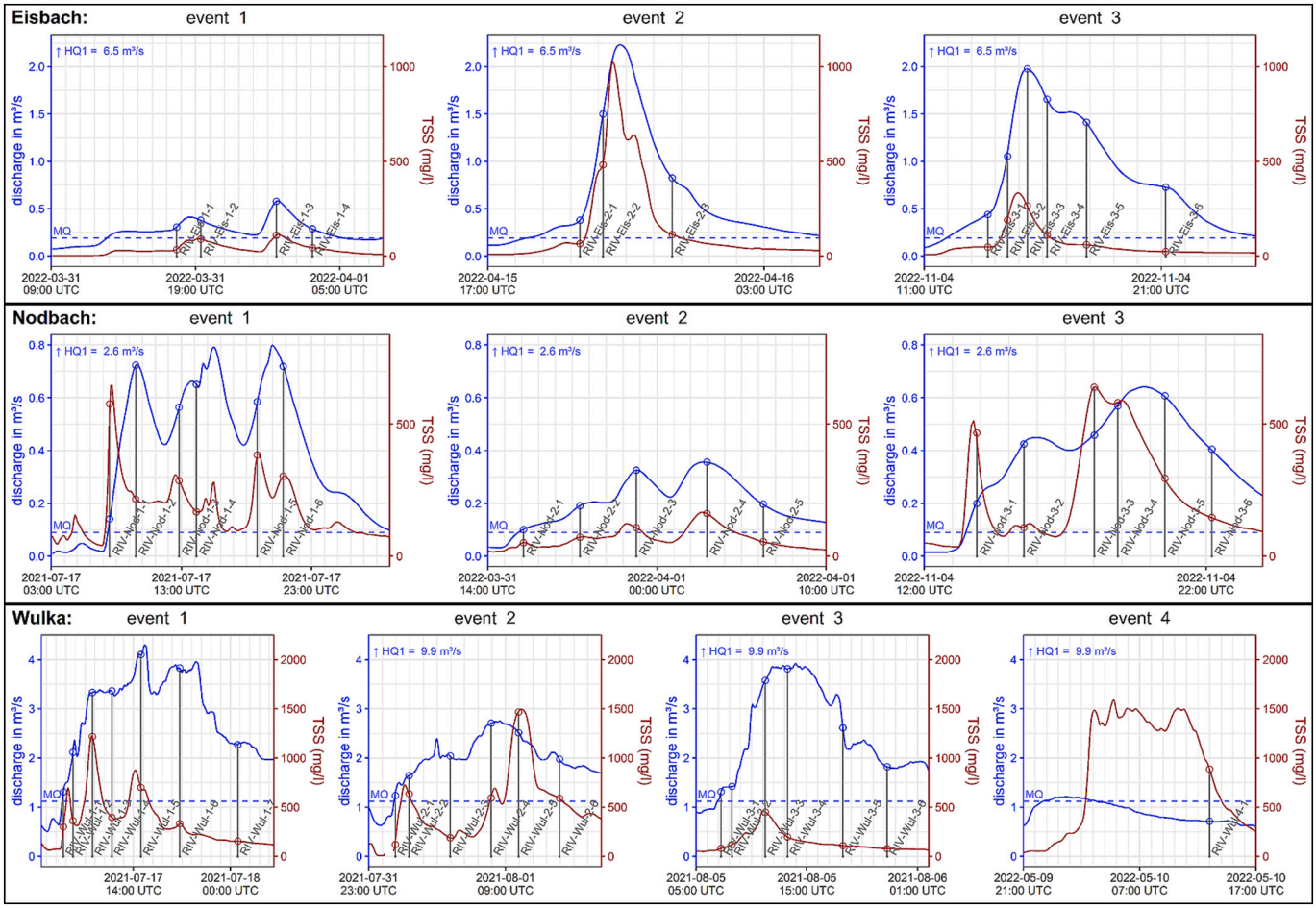


**Fig. 2.** Discharge (blue) and TSS-concentration (brown) dynamics (based on inline measurements) during the sampled events and time of sampling (indicated by vertical lines and circles at the intersections with the lines. Sample identifiers are noted above the abscissa. The mean annual discharge is indicated by dashed blue line, annual high-flow reported in the upper left corner. (For interpretation of the references to colour in this figure legend, the reader is referred to the web version of this article.)

according to DIN EN ISO 11905-1:1998-08 and P by ammonium molybdate spectrometric method according to DIN EN ISO 6878:2004-09. Unfortunately, in 8 event samples nutrients were not analysed, so the dataset is incomplete for N and P.

#### 2.3.2. *Determination of element concentrations and loss on ignition in soils and sediments*

Soil and sediment samples were homogenised, sieved (<2 mm) and lyophilised prior to analysis.

For element analysis approximately 0.2 g of lyophilized soil or sediment sample was weighed into a Teflon vessel and 2 mL of hydrogen peroxide, 4 mL of nitric acid, 1 mL of hydrochloric and 2 mL of hydrofluoric acid were added. The contents were subjected to microwave assisted digestion. After digestion, 12.5 mL of boric acid (4 % aqueous solution) was added to dissolve fluorides and complex the excessive boric acid and microwave assisted digestion was applied again. After digestion, the contents were transferred into 30 mL graduated PE-tubes and concentrations of elements (Li, K, Rb, Sr, Ba, Sc, Y, La, Ce, U, Ti, Zr, V, Nb, Cr, Mn, Fe, Co, Ni, Cu, Ag, Zn, Cd, Al, Ga, Tl, Pb, P, As, Sb, Bi, Se) were determined by ICP-MS, after appropriate sample dilution with ultrapure water. All the analyses were performed in triplicate.

Loss on ignition (LOI) as a proxy for organic content was analysed separately according to DIN 38409-2:1987-03. N was not analysed in soil and sediment samples, Sr und U were only analysed in soil and sediment samples but not in water samples. The analytical limits as well as the detection frequency are reported in Table S2 in the Supplemental Material.

### 2.4. *Data analysis*

We first describe the observed events and concentrations in event-flow and low-flow samples, then investigate the dynamics of the concentration within and between events and finally relate the concentration in SPM with the concentrations in bed sediment and soils in the catchment.

#### 2.4.1. *Software*

All data analysis was conducted in R 4.3.2 (R. Core Team, 2023) using mainly packages “data.table” 1.14.10 (Barrett et al. 2023), “ggplot2” 3.4.4 (Wickham, 2016), “ggrepel” 0.9.5 (Slowikowski, 2024), “NADA” 1.6 (Lee, 2020), “NADA2” 1.1.5 (Julian and Helsel, 2023) and “vegan” 2.6 (Oksanen et al. 2024).

#### 2.4.2. *Event hysteresis*

The first step in data analysis was to examine the sampled events based on the time series of discharge and TSS concentration derived from in-line water level and turbidity measurements. The hysteresis of TSS concentration and discharges was plotted and classified using hysteresis indices based on Lloyd et al. (2016) to compare events within and between catchments. A clockwise hysteresis, resulting from TSS concentration increasing more rapidly than discharge during the rising limb, indicates a sediment source close to the monitoring site while an

anticlockwise hysteresis, caused by a lag of the TSS concentration peak after the discharge peak, usually results from a sediment source further away from the monitoring site. The hysteresis index indicates the shape and strength of the hysteresis by comparing sections of the rising and falling limb of the event resulting in numbers between −1 (very strong anticlockwise hysteresis) and 1 (very strong clockwise hysteresis). In hysteresis events showing a figure of eight shape or more complex shapes, the different parts of the hysteresis may cancel each other out, resulting in hysteresis indices closer to 0 (no clear hysteresis shape) (Lloyd et al., 2016).

#### 2.4.3. Calculation of element concentrations in SPM

To exclude the influence of TSS concentration on the total concentrations, examine the quality of the transported particulate material and be able to compare it with soil and sediment concentrations, the element concentrations in suspended particulate matter (SPM) were derived as:

$$C_{i,SPM} = \frac{C_{i,total} - C_{i,dissolved}}{C_{TSS}} \cdot 10^3 \quad (1)$$

with $C_{i,SPM}$ being the concentration of element i in SPM (mg/kg), $C_{i,total}$ as total concentration of element i (µg/L), $C_{i,dissolved}$ as dissolved concentration of element i (µg/L) and $C_{TSS}$ as TSS concentration in the sample (mg/L). In cases where the dissolved concentration is below the limit of detection (LOD), the half value of the LOD is used. The maximal bias possibly introduced by this imputation with the half LOD value of dissolved concentration is 5 % of the total concentration, which we consider acceptable. In one sample, dissolved K concentration showed a slightly higher value than the total concentration, thus this would result in a negative concentration in SPM. In this case, the concentration was set as below the LOD.

### 2.5. Description of concentration levels and variability

Next, we describe the total and dissolved concentration levels observed in event flow samples, compare them to composite samples from low-flow periods and relate them to environmental quality standards to investigate the overall pollution level.

The concentration data were delivered by the laboratory reporting values for all measurements above the LOD, including for values below the limit of quantitation (LOQ). We consider the reported values between LOD and LOQ as associated with a higher uncertainty than values above the LOQ. However, such values might contain valuable information about the concentration level. Therefore, we only treat values below LOD as censored and use values between LOD and LOQ as they were reported. For handling censored data, suitable methods were applied wherever necessary following mainly the recommendations of Helsel (2011). For calculating statistical descriptors of position like mean and median, we apply "regression on order statistics" (ROS) to impute values below the LOD assuming a lognormal distribution of the data.

To measure and compare the variability contained in the data, a robust indicator is needed, which is not sensitive to single extreme values. The robust coefficient of variation (RCV) is used for this purpose, which is the quotient of median absolute deviation (MAD) divided by the median.

### 2.6. Investigating correlations and drivers during events

To investigate how concentrations evolve during events and what the driving forces might be, correlations between element concentrations on the one hand and time elapsed during the event, discharge at sampling time and TSS concentration of the sample on the other hand are tested. As for event 4 in the Wulka River there is only one sample available, this is excluded from this analysis as it would lead to an unbalanced data design. First, univariate correlations (one element per test) between the element concentrations and time or discharge or TSS concentration is tested using Kendalls τ. The "cenken" function from the NADA package is applied to adequately consider censored values. Correlations are considered statistically significant if their *p*-value is below 0.05.

Second, we investigate the multivariate case (all elements at once), to see which of the three drivers, which are auto-correlated adds most to explaining the development of variability of water quality during events. To do so the left censored concentration data are first transformed into a distance matrix by calculating the Euclidian distances of the ranks of their u-scores (Helsel, 2011). This distance matrix is used to test the significance of discharge, TSS concentration and time since event onset in explaining the variability in the distance matrix by application of PERMANOVA (Anderson, 2014) using the "adonis2" function from the "vegan" package. PERMANOVA is a permutation test, which means that it does not require an assumption about the distribution of the data. The test is performed by comparing the data as given with the data after permutating samples for the null hypothesis that there is no significant effect. As we assume, that at least some events might be significantly different than others (also tested with PERMANOVA resulting in $p = 0.001$), we use an event identifier to define strata during the permutations test, which suppress sample permutation between different events in the multivariate test. Events are defined per sampling sites, so this also suppresses permutation of samples between different sampling sites. The test is applied assessing the marginal effects of each variable (time, discharge, TSS concentration) in a model with the other variables already included to see if this variable significantly adds to explaining the water quality. This test is done for total concentrations, dissolved concentrations, SPM-concentrations and each of them only for PTE.

### 2.7. Comparison of events

Following the investigation of dynamics during events it is tested if different events show significant differences and if there are variables available which explain them. Again, a PERMANOVA test is applied including discharge during sampling, the TSS-concentration and an event identifier as independent variables and test them for their relations with the distance matrix of the concentrations (derived as explained above). As the three sampling sites are considered different in their characteristics, they are used as strata in the test supressing sample permutations between the sites. While the PERMANOVA test is not sensitive regarding the underlying distribution of the data it requires homogeneity of dispersion for groups of data defined by categorical variables as the event identifier in this case. Therefore, we tested, if the underlaying assumption of homogeneity of dispersion must be rejected by applying the PERMDISP test (function "betadisper" from "vegan" package) before applying the PERMANOVA test. With *p*-values of 0.72 (total), 0.53 (dissolved) and 0.57 (SPM) homogeneity of dispersion in events (the fourth event from Wulka was excluded again) could not be rejected and the PERMANOVA test can be applied.

Next it was tested if the length of the period between a previous event and the sampled event has a significant relation with the multivariate concentration data. Again, a PERMANOVA test is applied including discharge during sampling, the TSS-concentration and two variables for the pre-event dry period: The number of days since a (smaller) event occurred and the days since an event with the same or higher discharge magnitude occurred. Again, the three sampling sites are used as strata in the test supressing sample permutations between the sites. With *p* values clearly above 0.05 in the PERMDISP test for all constellations homogeneity of dispersion could not be rejected and the PERMANOVA procedure could be applied.

As a post hoc test Kendall's τ correlation test is applied to test correlation between each of the time variables and each of the substances.

### 2.8. Relation between SPM quality, riverbed sediments and soil in the catchment

The comparison of calculated concentrations in SPM with the potential particulate matter sources in the catchment – bed sediments and soils – are conducted by deriving element enrichment factors (EF), as this allows for visualization of all elements on the same scale. First, elemental enrichment was examined against reference materials such as the upper continental crust (Taylor and McLennan, 1995) or global SPM data (Viers et al., 2009) to identify elements that show anthropogenic changes in their occurrence. As the calculated enrichment factors showed very high enrichment/depletion in all samples of all compartments for some elements (see Figs. S7 and S8), it was concluded that for those elements local geochemistry might be different from global values and thus a local material is needed to investigate anthropogenic enrichment and depletion effects (cp. Reimann and de Caritat, 2000). As the soil samples showed very stable concentrations for most elements, which can be explained by the approach of collecting spatial composite samples, the median of soil concentration of all samples was tested as reference concentration. Thus, the enrichment or depletion values calculated here show comparison to average soil concentrations in the catchment. To control for dilution effects caused by major phases such as carbonates, silicates or organic material, which can occur due to changes in grain size during erosion, transport and sedimentation processes, concentrations were normalized using the Al content, as recommended by Chen et al. (2014). This is because Al is an important insoluble constituent of clay minerals and is hardly enriched or depleted significantly by human activities.

$$EF_i = \frac{C_{i,sample}}{C_{Al,sample}} \cdot \frac{med(C_{Al,soil})}{med(C_{i,soil})} \quad (2)$$

with $EF_i$ being the enrichment factor of element i in a solids sample, $C_{i,sample}$ the concentration of element i in the sample, $C_{Al,sample}$ the Al concentration in the sample, $C_{AL,soil}$ the Al concentration in local soil and $C_{i,soil}$ the concentration of element i in local soil. Values below LOD were imputed with half value of LOD in this step, leading to some very low EF values (high depletion). Especially the one sample where K was measured with higher dissolved than total concentration yielded a very low EF, which was considered implausible and therefore removed from the visualization.

To test if relations between element concentrations in SPM event samples, sediment and soil can be established, which would point to specific sediment sources in the catchment, nonmetric multidimensional scaling (NMDS) was applied for dimension reduction. A distance matrix was derived using euclidian distances of ranks of u-scores of the concentrations to properly handle censored data. The function "metaMDS" from the vegan package was used to generate the NMDS with the "monoMDS" engine.

### 2.9. Derivation of enrichment ratios for soil erosion modelling

Enrichment ratios for modelling substance emissions into surface waters by soil erosion are derived based on Sharpley (1985) but using the median for aggregating the concentrations, as this is more robust against outliers:

$$ER_i = \frac{med(C_{i,SPM})}{med(C_{i,soil})} \quad (3)$$

with $ER_i$ being the enrichment ratio for element i. As the enrichment of fine particles and change in mineralogical composition (enrichment of clay and organic matter) should be depicted by these ratios, no correction is applied here. The soil concentrations from the sampling of arable land were used to derive the enrichment ratio, as arable land is the major land use in the catchment and the enrichment ratios are mainly applied for modelling substance emissions into surface waters by soil erosion from arable land. Regarding the SPM concentrations, the samples from Eisbach were excluded, as urban impact dominates in this subcatchment over soil erosion.

## 3. Results and discussion

The following section first characterises the sampled events, then compares the concentration levels in event-flow samples and baseflow samples, as well as in soil and sediment samples, and relates them to environmental quality standards. The concentration variability is then presented and used to investigate dynamics during and between events. This is followed by the description and discussion of element enrichment in SPM, soil and sediment. Finally, the results of testing whether a sediment fingerprinting can be derived with the available data and the estimated element enrichment ratios are presented.

### 3.1. Event characterisation

The 10 sampled events from 3 catchments can be classified as strong events regarding TSS concentration and discharge (Eis-2, Nod-1, Nod-3, Wul-1, Wul-2), strong only regarding discharge (Eis-3, Wul-3), strong only regarding TSS concentration (Wul-4) and generally weaker events (Eis-1, Nod-2). All automatically sampled events (exception is Wul-4) were sampled over different stages of the event including samples from the rising as well as from the falling limb.

The Eisenstadt WWTP discharges treated wastewater into the Eisbach. During storm events, the maximum inflow volume into the plant is 0.563 $m^3/s$ (Abwasserverband Eisenstadt-Eisbachtal, 2025). This could have had a significant impact on the samples taken in the lower discharge reach. In particular, the samples from the first event at Eisbach, which were collected at a relatively low discharge rate of 0.29–0.58 $m^3/s$, are likely to be significantly affected by treated wastewater.

To better characterise the sampled events, hysteresis plots of TSS concentration versus discharge (Fig. 3) are used. Almost all events show mainly clockwise hysteresis or complex hysteresis patterns, only the fourth event at Wulka has a clearly anticlockwise hysteresis shape.

Even if the catchments are of limited size, the complex hysteresis patterns point to overlaying flow waves from different precipitation events in different tributaries and regions of the catchment. While the Nodbach has the smallest catchment and lowest flow during dry weather, it shows quite complex hysteresis patterns. The hysteresis always starts clockwise pointing to a close-by sediment source. This source might be located in a small side arm coming from a village, where impervious areas are connected via storm sewers and a retention basin to the Nodbach. The first event at Eisbach with its complex and slightly anticlockwise hysteresis is in a comparable low discharge and TSS range, here the input of treated wastewater might explain most of the shown effects. The other two events at Eisbach show clockwise TSS-discharge hysteresis patterns during rather short events, probably caused by fast runoff from sealed urban areas. Wulka river, which has a much larger catchment including Nodbach and Eisbach tributaries, shows stronger hysteresis indices as the tributaries, with mainly clockwise hysteresis shapes but also one clear anticlockwise hysteresis event, which was unfortunately only sampled with one sample. This anticlockwise hysteresis with a relatively slow decline of the TSS concentration might indicate a soil erosion event, as indicated by Williams (1989).

### 3.2. Comparison of concentration levels

Looking at the concentrations of PTEs during event-flow in comparison to base-flow (Fig. 4), it is apparent that total concentrations during event-flow are higher than during low-flow periods. This is highly significant for Nodbach and Wulka for all PTE while for Eisbach all PTE show the same pattern but differences are less severe and for Ni

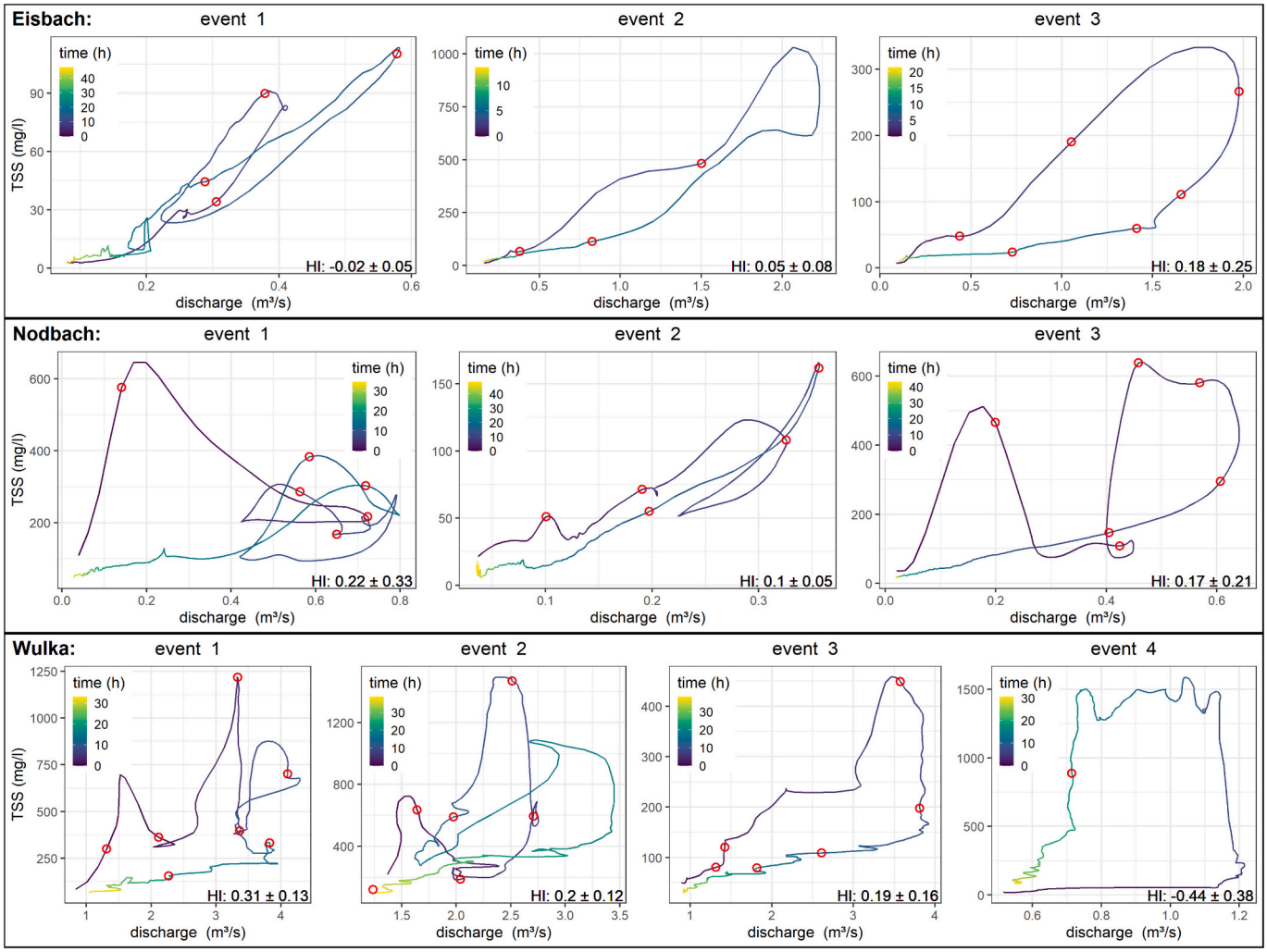


**Fig. 3.** Discharge vs. TSS concentration hysteresis of the events based on inline data. The line colour from blue to yellow indicates time after beginning of the event. Red circles indicate the time when samples were taken. Hysteresis indices based on Lloyd et al. (2016) are reported in the lower right corner. Note the differences in axis scaling of the plots. (For interpretation of the references to colour in this figure legend, the reader is referred to the web version of this article.)

differences are not statistically significant.

The up to one order of magnitude higher concentrations during events, especially for Pb, Cr, Cu, Zn, and Cd, support the known importance of event-flow for catchment export of PTEs (Ciszewski and Grygar, 2016; Milačič et al., 2017).

When comparing the dissolved concentrations during event and low-flow, the levels differ less than for the total concentrations. Only Cu shows significantly higher dissolved concentrations in event-flow, which might stem from wash-off from soil in vineyards, where elevated concentration might be caused by Cu application as fungicide in viticulture (Cesco et al., 2021). In this fungicide, Cu is present in the form of highly water-soluble $CuSO_4 \times 5H_2O$, which is highly mobile in the soil and easily leaches into river water. The hypothesis of viticulture being the source for dissolved Cu is further supported by the finding that Cu concentrations in soil of vineyards (80 ± 5.8 mg/kg) were significantly higher (one sided Wilcoxon-test, $p = 0.022$) than in soil of other land use (20.8 ± 7.4 mg/kg). Nevertheless, other sources, e.g. Cu application as fungicide for wood preservation (Gomez Cortes et al., 2022) in settlements, may also contribute to the elevated dissolved concentrations. As the Eisbach sub-catchment, which shows the highest dissolved Cu concentrations, has both the largest areas of viticulture and urban areas, it is not possible to differentiate in this study.

To contextualise the observed contamination levels in terms of their toxicity and relevance to water quality management, they are compared with environmental quality standards (EQS): Dissolved concentrations of Ni, Cd and Pb can be compared with the EU environmental quality standards (EQS, EU, 2013) and are found in all samples clearly below those thresholds (both the maximum allowable concentration EQS as well as the annual average EQS). Cu, Zn are well below local EQS values (Amann et al., 2019), which consider the influence of water hardness. For As no applicable EQS exist, but AA-EQS values from other countries are found between 4.4 and 25 µg/L (Durjava et al., 2013), where the lowest one (4.4 µg/L from France) is only slightly exceeded by 4 event-flow samples. For Cr no EQS value is applicable (Vaiopoulou and Gikas, 2020). The dissolved concentrations of thallium, another very toxic metal, is around the LOD of 5 ng/L and thus in the lower range of unpolluted freshwater bodies (Zhuang and Song, 2021). Therefore, the overall level of PTE concentration in the studied catchment is low to moderate and no exceedance of EQS values is detected. The environmental relevance of PTEs therefore is mainly given due to Wulka being the main tributary to lake Neusiedl and the potential enrichment in sediments and water column of this endorheic lake. In this respect dissolved and particulate forms have to be considered as PTEs particle bound PTEs might be mobilised under lake conditions.

A comparison of total and dissolved concentrations of all other investigated elements in event-flow samples (for which no low-flow values are available for comparison) can be found in Fig. S1.

The element concentrations in soils and sediments were always in the

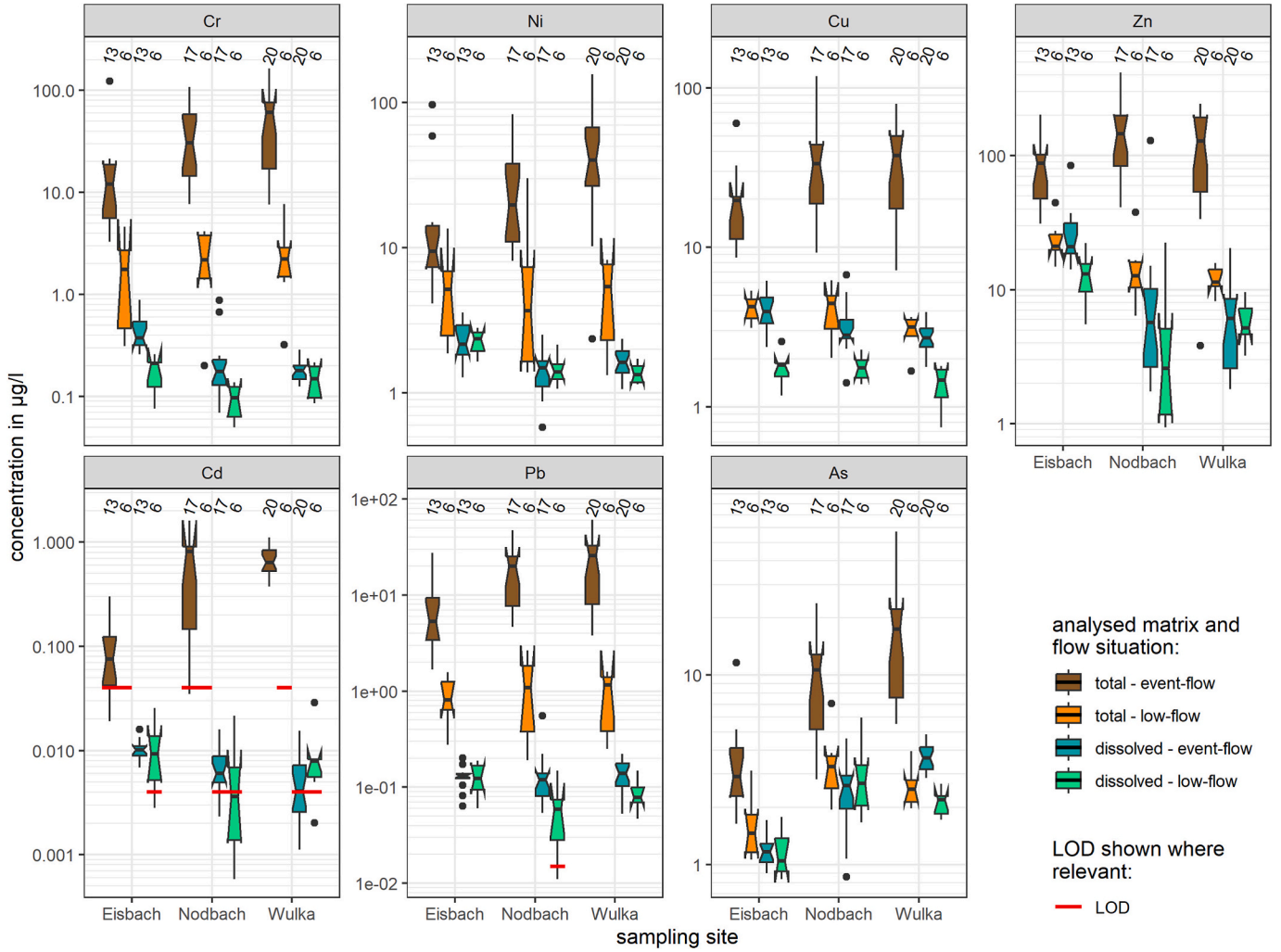


**Fig. 4.** Concentrations (total and dissolved) of potentially toxic elements in event-flow and low-flow samples from the three rivers. Notches in the box plots indicate confidence interval of the median. Values below LOD were imputed by ROS method if at least 20 % of the measurements and 3 values were above the LOD. Where the boxplot is missing, e.g. Cd total concentrations during low-flow, too many values were below LOD. The LOD is indicated as red line where relevant. (For interpretation of the references to colour in this figure legend, the reader is referred to the web version of this article.)

same order of magnitude, often with slightly higher median concentrations in soil (Fig. S2).

### 3.3. Investigation of concentration variability and possible drivers

Variability of concentrations between the different samples is the basis for all further statistical evaluation of the event concentration data. Therefore, Fig. 5 shows the overall variability of the concentrations for the different elements in different environmental compartments (river water and SPM during events, riverbed sediment, soil) and analysed matrices of water (total and dissolved), represented by the RCV.

Generally, lowest variability can be seen in the soil data, which is not unexpected as they were created as spatial composite samples aiming for representativeness of different land use types. Therefore, the elevated variability for Cu is noteworthy, which is due to elevated Cu concentrations in soil samples from vineyards, as already mentioned and discussed above. Riverbed sediments show higher variability than soil samples and mostly lower variability than event-flow total concentrations. Dissolved concentrations in event-flow samples are mostly less variable than total concentrations, with the exception of Mn, Zn and Bi. The high variability of dissolved Sb, La and Ce is also noteworthy.

The variability of the total element concentrations is of similar magnitude as the variability of TSS (RCV = 0.63). To determine how much of this variability is due to variability in TSS content alone, the RCV of concentrations in the SPM was calculated. For most elements, the variability of SPM content is significantly lower than that of total concentrations, which indicates that a major share of variability is only caused by TSS concentration dynamics. Some exceptions, like for instance for Sb, Bi and Cd, show however high variability in SPM even if slightly reduced compared to total concentrations, indicating that other factors than the magnitude of SPM transport might play a role in their dynamics.

### 3.4. Dynamics during events

To investigate the dynamics of individual elements during events, we tested whether there was a correlation of total and dissolved concentration in water and concentration in SPM with the time elapsed during the event, the discharge during sampling or the TSS concentration of the sample. All $\tau$ and $p$ values of Kendall's $\tau$ correlation tests are reported in Table S3.

All total element concentrations show significant and strong positive correlations with the TSS concentration except for Sb, which is showing a different behaviour. This supports the well-known fact that during event flow the particulate transport is highly relevant for most elements. For selected elements the correlation of the total concentration with the

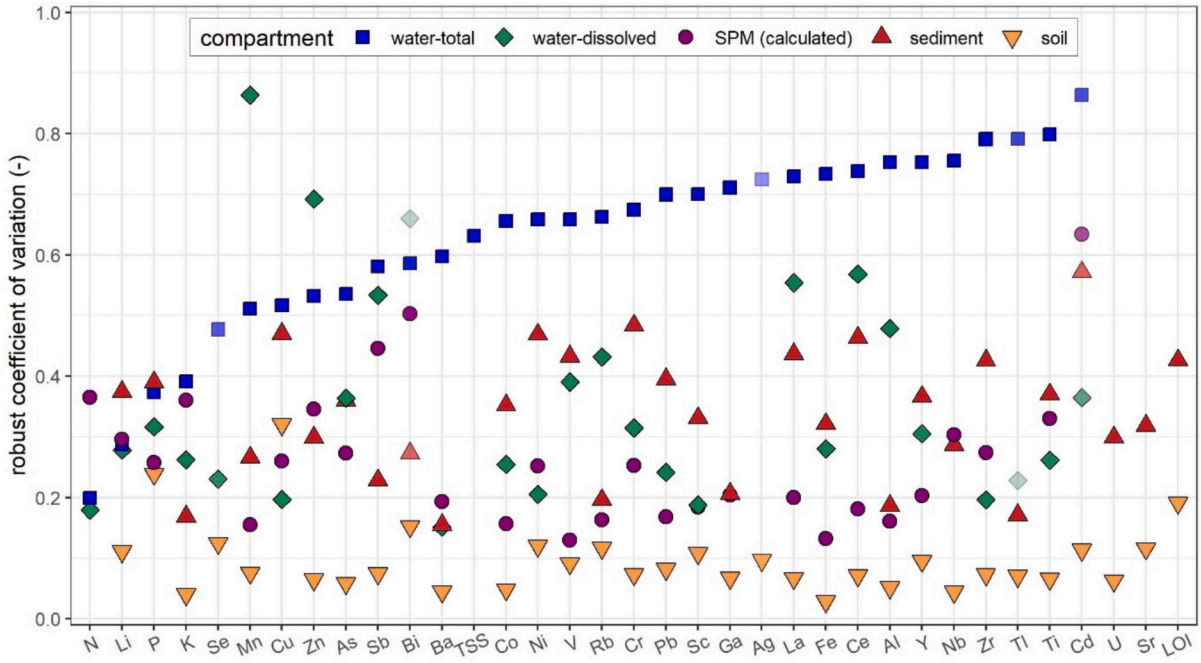


**Fig. 5.** Variability of different parameters in different environmental compartments and analysed matrices: Variability is presented by the robust coefficient of variation. Detection rate is indicated by transparency of the symbols, higher transparency indicates lower detection rate (share of values above LOD). Elements are ordered from low to high variability of total concentration in event-flow samples. U, Sr and LOI were not analysed in event-flow samples. For Se, Ag and Tl no RCV of SPM and sediment concentrations could be derived because to many values were below LOD.

TSS concentration is plotted in Fig. S3, which allows direct comparison with the results of Nasrabadi et al. (2016). The correlations found here are still weaker than those shown in Nasrabadi et al. (2016), meaning that the proposal of using TSS concentration as proxy for PTE concentrations would not give so meaningful result for the situation studied here. The correlation with the discharge is also significant and positive for most elements, but less strong than that with TSS. Exceptions are Bi, Cd, Li, Mn, Zn and Ag, which are not significantly correlated with discharge. Only few elements show a significant correlation with time elapsed during the event: Sb, Bi, K, Ag and Zn are negatively correlated with event time. These correlations are weaker and less significant than correlations with TSS concentration for Bi, K and Zn. Only for Sb and Ag these are the strongest correlations found for total concentrations.

With regard to the dissolved concentrations, patterns are less pronounced. Positive correlations are found between TSS concentration and dissolved Pb, Tl, Y, As, Ce, La, Ti, and V, while dissolved Rb and Zn are negatively correlated. Positive correlations with the discharge are shown for dissolved Pb, Sb, Y, Al, As, Ce, La, Ti and V, while dissolved Cu, Mn and Zn are negatively correlated. The time elapsed during the event is negatively correlated with dissolved concentrations of Zn, Co, Rb, K, Sb, Bi and Nb and positively correlated with dissolved Ce. The strong positive correlation of dissolved concentration of As, Y and rare earth elements Ce and La with discharge might be interpreted as mobilisation of geogenic components by increased interflow from the vadose zone due to rainwater infiltration, as reported by Barber et al. (2017) for an extreme flood.

By examining the calculated concentrations in the SPM, it is possible to exclude the direct influence of the TSS concentration and identify which drivers other than the SPM transport are relevant. The results indicate mixed correlations of SPM element concentrations with the TSS concentration, with positive correlations shown for Ce, K, La, Ti, Tl, Y, Al, Zr and Rb, and negative correlations for Bi, Cu, Mn, Sb, Zn and Li. Similar mixed correlations are found with discharge, namely positive for Ba, Ce, Ga, La, Nb, Ti, Y, Al, F, Rb and Zr, and negative for Bi, Cu, Mn, Zn and Li. In general, this can be interpreted as a shift from anthropogenically impacted elements at lower discharge and TSS levels to more lithogenic elements at higher levels of TSS transport and discharge, as also reported by Matsunaga et al. (2014). For Sb and Cu there is also a significant negative correlation between element concentration in SPM and event duration, i.e. higher concentrations at the beginning of events. This can be explained by a higher proportion of SPM from roads at the beginning of events, which is quickly flushed into rivers via road runoff through storm drains and contains Sb and Cu from abrasion of brake wear particles (Philippe et al., 2023) and other traffic-related sources (Taylor and Kruger, 2020). As the events progress, the easily flushable road dust source may be depleted, resulting in a shift towards a greater proportion of less contaminated soil material in the SPM.

As shown above, for several elements not only one of the drivers (discharge, TSS concentration or time) shows significant correlations, but two or even three of them, which is not unexpected as they are partially correlated. To test whether all three drivers contribute significantly to the explanation of concentration variability during events, we applied a multivariate PERMANOVA test with discharge, TSS concentration and time since event onset as explanatory variables and substance concentrations as response variables. The results of the different tests are shown in Table 2.

For total and dissolved concentrations all three potential drivers

**Table 2**
Results of PERMANOVA test (test statistic F and *p*-value) for different drivers explaining event concentrations during events in different subsets of concentration data using the marginal contribution of each variable. Not significant test results are printed in italic.

| Concentrations | Discharge | | TSS concentration | | Time since event begin | |
|---|---|---|---|---|---|---|
| | F | p | F | p | F | p |
| All elements - total | 5.16 | 0.0031 | 50.35 | 0.0001 | 4.41 | 0.0040 |
| All elements - dissolved | 4.96 | 0.0178 | 4.88 | 0.0179 | 5.03 | 0.0001 |
| All elements - SPM | 5.49 | 0.0424 | *2.64* | *0.0946* | *2.35* | *0.1002* |
| Only PTE - total | 3.99 | 0.0002 | 37.32 | 0.0001 | 6.45 | 0.0004 |
| Only PTE - dissolved | *3.74* | *0.2560* | 8.11 | 0.0001 | 6.16 | 0.0001 |
| Only PTE - SPM | *2.72* | *0.4537* | 4.49 | 0.0011 | 3.29 | 0.0084 |

show highly significant contributions to explaining variability, for the SPM concentrations only the discharge contributes significantly. Interestingly, this is different when only PTE concentrations are examined in the test, where discharge does not contribute significantly to the explanation of dissolved and SPM concentrations, but TSS concentration and time elapsed since event onset are significant. The strong relationship between discharge and trace element concentrations in the SPM may indicate that different types of particulate matter are transported depending on the amount of discharge, as also reported by Pulley et al. (2016) and Matsunaga et al. (2014).

### 3.5. Quality differences of events and underlying factors

The PERMANOVA test, for at least one event with concentrations significantly different from the others after accounting for discharge and TSS variability, is not significant at the 0.05 confidence level for total concentrations and SPM, but highly significant for dissolved concentrations (Tables 3 and 4).

This indicates that, after excluding the effects of variations in discharge and TSS concentration on the elemental composition, only the dissolved phase differs significantly in composition between some events. It can be presumed that the high variability of TSS concentration masks minor patterns in the variability of total and SPM concentrations.

To investigate further drivers determining the concentration patterns of events aside from discharge and TSS concentration, the time elapsed since the previous event at the same location was tested. The p-values of the test for marginal effects of the variables are presented in Table 4, showing that both the time since the last small event, but especially the time since the last event with the same discharge magnitude, have significant explanatory power for the variability of the concentrations.

A possible explanation for this behaviour is the build-up of storages in the catchment, either by atmospheric deposition and traffic emissions on unsealed soils and sealed surfaces, or in the riverbed by temporary sedimentation, which are then mobilised under event flow conditions. The longer the period of accumulation, the higher the level of storage and the more that can be mobilised.

As univariate post hoc test, Kendall's tau correlation was applied for both time variables: For the time since the last (smaller) event, numerous strong ($|\text{tau}| > 0.3$) and significant ($p < 0.05$) correlations were found. Total concentrations of Ti, Nb, Y, As, Ce, V, La, Rb, Zr, Al, Ga, Sc, Fe, Ba, Co, dissolved concentrations of As, La, Ce, Y, V, and SPM concentrations of Ti, Y, Nb, La, Ce and Rb correlated negatively with the pre-event period duration, while dissolved concentrations of Cd, Zn and Mn and SPM concentrations of Li, Cu, Mn, Zn and Bi correlated positively. For the time since an event of equal or greater discharge magnitude, correlations were positive for total concentrations of Bi and Cd, dissolved concentrations of Se and Tl, and SPM concentrations of Tl, Pb and Cd, while a negative correlation was found for dissolved Sc (for detailed test results see Table S4).

**Table 3**
Results of PERMANOVA test (test statistic F and p-value) for different drivers explaining event concentration differences between events in different subsets of concentration data using the marginal contribution of each variable. Not significant test results are printed in italic.

| Concentrations | Discharge | | TSS concentration | | Event ID | |
|---|---|---|---|---|---|---|
| | F | p | F | p | F | p |
| All elements - total | *3.36* | *0.0753* | 23.64 | 0.0001 | *3.22* | *0.0758* |
| All elements - dissolved | 4.93 | 0.0060 | 10.51 | 0.0001 | 4.96 | 0.0001 |
| All elements - SPM | *1.95* | *0.1460* | *2.27* | *0.1045* | *1.94* | *0.1043* |

### 3.6. Relation between SPM quality, riverbed sediments and soil in the catchment

The enrichment and depletion of elements in SPM and sediment against median concentrations in local soil are shown in Fig. 6.

All elements with a strong enrichment in SPM compared to the local soil (Ag, Bi, Zn, Cu, P) show the highest enrichment for Eisbach, followed by Nodbach and Wulka. The sediments show no enrichment for these elements. For Cd the highest enrichment is found in a few samples from Wulka, followed by a clear enrichment in all samples from Nodbach. The high depletion shown for Wulka results from values below LOD. Sb interestingly shows strong enrichment in Eisbach SPM and only in a few samples from Nodbach and Wulka. At the other end of the spectrum, depletion of Zr and Ti can be observed in SPM and to a lower extent in sediments.

The high enrichment of Ag, Bi, Zn, Cu, P, Sb, Ni and Li, especially in the Eisbach, indicates emissions of these trace elements from urban activities. All these elements have many applications in the technosphere and thus emissions via untreated and maybe also treated wastewater from urban areas are a likely source. Bi and Sb show the highest enrichment: Bi is used in pharmaceuticals, cosmetics and as pigment in weatherproofed paintings, while Sb is used in brake linings of cars and thus emitted in significant amounts. The findings indicate an apparent contradiction, namely that the enrichment in samples from Nodbach is higher than in those from Wulka, while the anthropogenic pressure in Wulka (emissions of treated wastewater, share of urban area, population density) is higher than in Nodbach. Interestingly the enrichment of Cd in Eisbach is lower than in Nodbach and some samples from Wulka, which is not in line with the aforementioned group of elements. A founded and plausible interpretation for these observations is not available.

The depletion of Zr and Ti indicates classification processes during solids mobilisation and transport: Heavy minerals contain these elements, e.g. zircon containing Zr and rutile containing Ti, and thus the element ratio between Zr and Al (slopes of the correlations in Fig. 7) can be used as indicator for such heavy mineral content (Chen et al., 2014). SPM generally contains lower Zr content than sediments and especially than soil. One extreme outlier with very high Zr content can be observed. Interestingly this outlier does not occur for Ti, which generally shows the same pattern. One explanation for the depletion of these elements is that due to the higher density of their minerals, they are not well mobilised in the soil erosion process and, when they reach the river, are deposited in the bed sediments rather than being held in suspension.

To test if relations between element concentrations in SPM event samples, sediment and soil can be established, which would point to

**Table 4**
Results of PERMANOVA test for marginal effect of a variable having all other variables included in the model. Not significant test results are printed in italic.

| Concentrations | Discharge | | TSS concentration | | Days since last event | | Days since last same size or bigger event | |
|---|---|---|---|---|---|---|---|---|
| | F | p | F | p | F | p | F | p |
| All elements - total | *3.37* | *0.21* | *2.51* | *0.12* | 3.21 | 0.003 | 4.37 | 0.0006 |
| All elements - dissolved | *2.22* | *0.21* | 44.0 | 0.0001 | *3.86* | *0.06* | 4.94 | 0.026 |
| All elements - SPM | *2.58* | *0.46* | *2.23* | *0.09* | 3.76 | 0.014 | 4.06 | 0.02 |
| Only PTE - total | *1.82* | *0.42* | 31.65 | 0.0001 | *2.33* | *0.12* | 7.62 | 0.002 |
| Only PTE - dissolved | *2.62* | *0.31* | 4.40 | 0.01 | 2.74 | 0.039 | 3.48 | 0.0003 |
| Only PTE - SPM | *2.48* | *0.41* | 3.54 | 0.02 | *2.52* | *0.058* | 8.52 | 0.0004 |

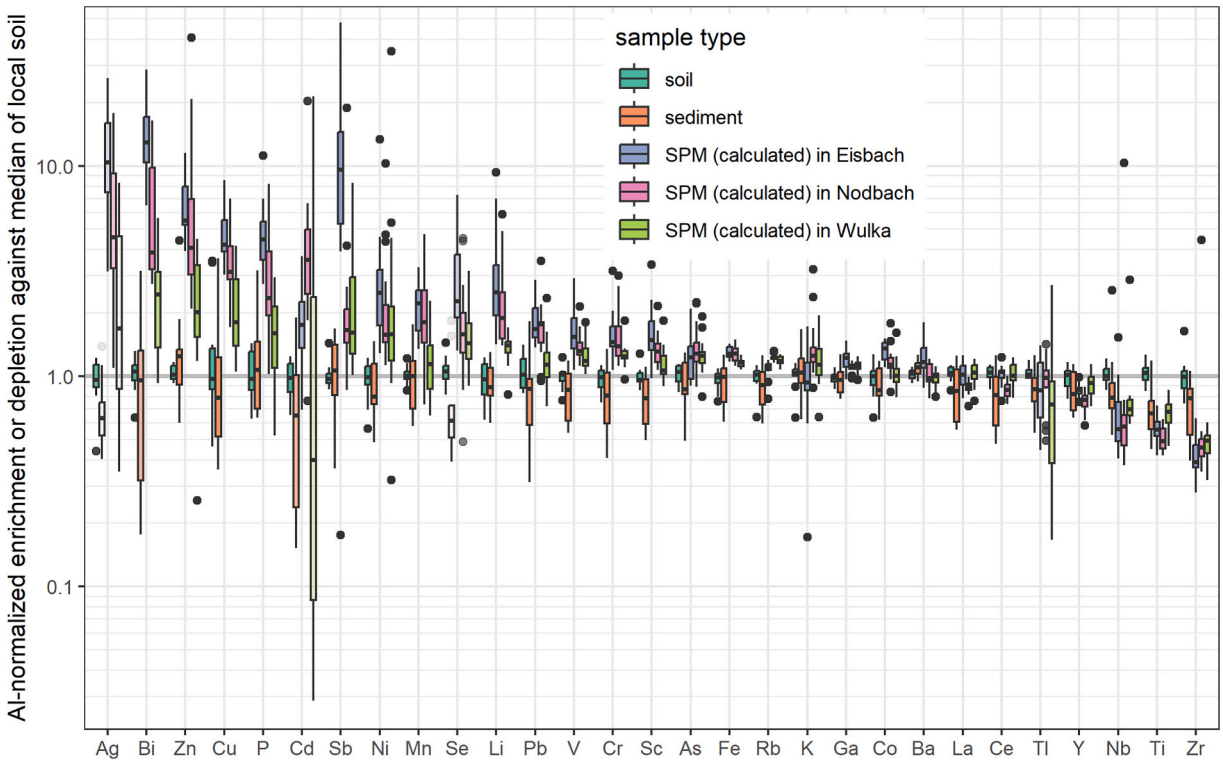


**Fig. 6.** Element enrichment or depletion in SPM (calculated) and in riverbed sediments against the median composition of local soil. Normalization with median Al content was applied to reduce grainsize effects. Transparency of boxplots indicates share of values below LOD. Elements are ordered according to decreasing enrichment factors of SPM (from all sites). Values below LOD were imputed with LOD/2 and share of values below LOD is indicated by transparency of boxplots.

sediment sources in the catchment, a nonmetric multidimensional scaling was applied for dimension reduction and plotted to examine the clustering of samples (Fig. 8).

From the first two dimensions of the NMDS it can be seen that the variability in the quality of the event samples is comparably high, even for samples from the same site and event. Very few samples show very

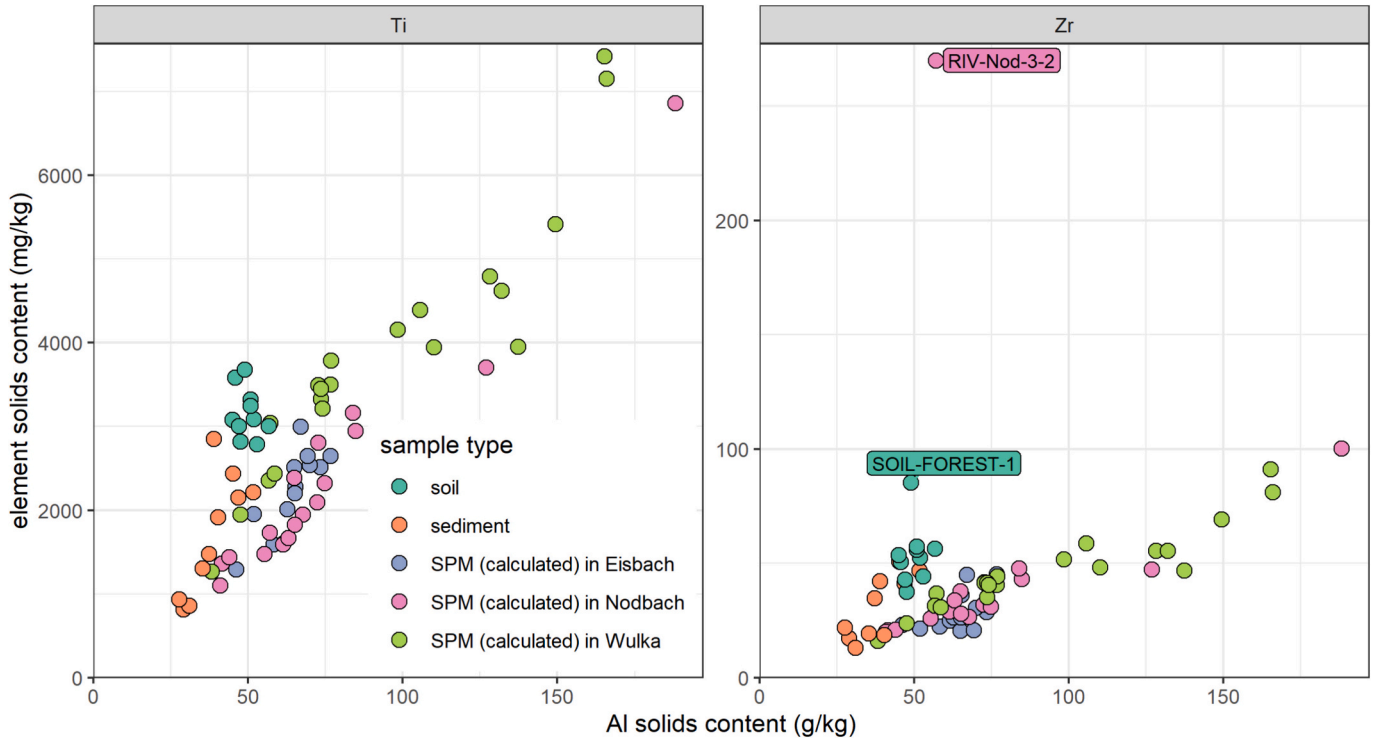


**Fig. 7.** Concentrations of Zr and Ti plotted against concentration of Al for soil, sediment and SPM.

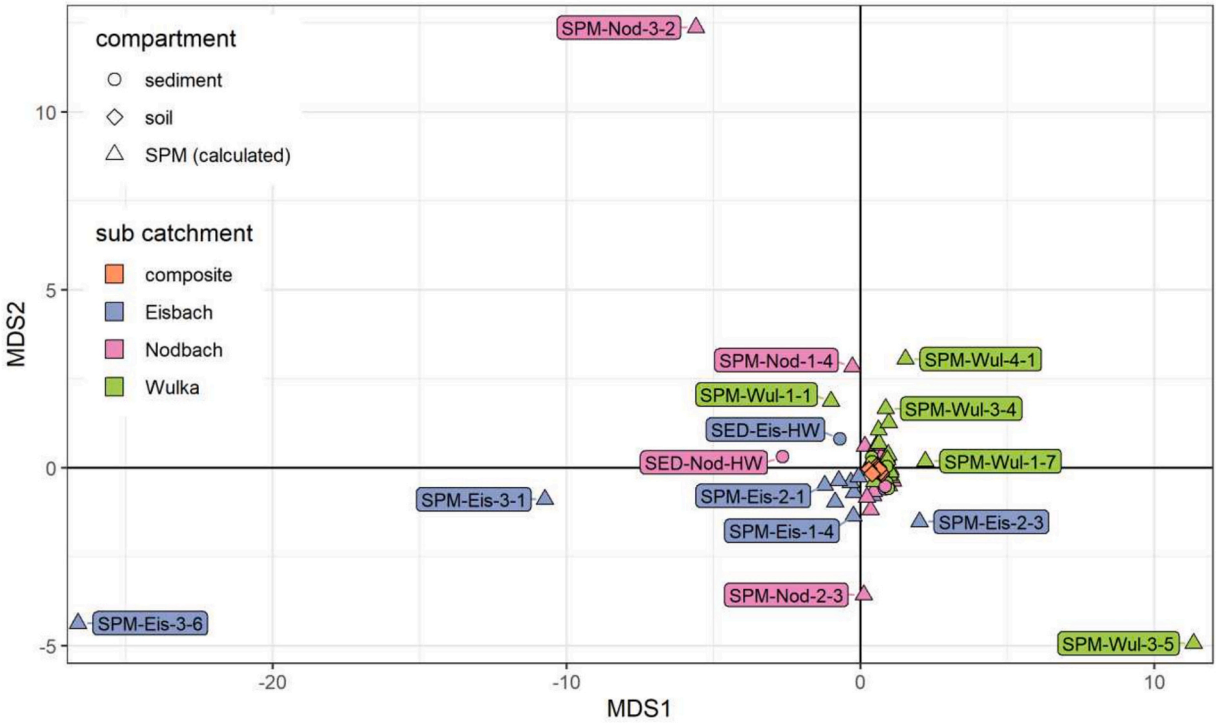


**Fig. 8.** First two dimensions of Nonmetric Multidimensional Scaling (NMDS) for element concentrations in SPM (calculated), sediment and soil. Labels show sample IDs.

**Table 5**
Element enrichment ratios (ER) for the combined process of soil erosion and sediment export with comparison to literature values.

| Element | This study | Auerswald and Haider, 1992 | Fuchs and Schwarz, 2007 | Quinton and Catt, 2007 |
|---|---|---|---|---|
| Bi | 4.7 ± 1.0 | | | |
| Zn | 4.3 ± 1.0 | | 1.6–3.5 | |
| Cd | 3.5 ± 2.0 | | 1.2–3.5 | |
| Cu | 3.4 ± 0.2 | 1.2–2.7 | 1.4–5.0 | 3.98 ± 0.16 |
| Sb | 2.9 ± 0.8 | | | |
| Ni | 2.5 ± 0.4 | | 1.3–4.8 | 3.01 ± 0.10 |
| P | 2.5 ± 0.1 | 0.9–1.9 | 1.1–2.5 | |
| Pb | 2.3 ± 0.3 | | 1.0–3.6 | 3.27 ± 0.14 |
| Mn | 2.2 ± 0.0 | | | |
| Cr | 2.0 ± 0.3 | | 1.7–5.5 | 2.1 ± 0.08 |
| As | 1.9 ± 0.5 | | | |
| V | 1.9 ± 0.1 | | | |
| Co | 1.7 ± 0.2 | | | |
| Tl | 1.3 ± 0.5 | | | |

distinct composition, while most of the samples cluster closer together and are not very different from riverbed sediment and soil material. Of the riverbed sediment samples, only two stand out (SED-Eis-HW and SED-Nod-HW), both from the upper reaches of the rivers, where the riverbed consists less of deposited sediments and more of autochthonous soil. All other sediment samples cluster very close together with the soil composite samples and many of the SPM event samples. Thus, it is not possible to establish a relation between single event samples and certain sediment or soil samples, which could be interpreted as source attribution for the SPM. The reason for this might be the sampling approach with rather few samples from soil and bed sediment.

Finally, element enrichment ratios were derived from the soil and SPM concentrations as input for emission modelling of pollutants into surface waters by soil erosion. The enrichment ratios are shown in Table 5 and compared with literature values where available. The high uncertainty for the Cd enrichment ratio derives from significant differences in the SPM concentrations from Wulka and Nodbach. For Wulka the enrichment ratio is 0.9 ± 0.1 (with 59 % of the SPM concentrations below LOD) while for Nodbach 4.8 ± 1.7. These differences are probably the effect of a mixture of variability of catchment characteristics and uncertainty stemming from censored observations.

The ER depends on the intensity with which fine and organic particles are enriched during soil loss, and thus on the intensity of soil loss (Sharpley, 1985). The more intense the soil loss, the lower the expected ER. The events sampled in this study were comparably small, resulting in limited soil loss and likely hight enrichment of fine and organic particles in SPM compared to the soil. Therefore, the high ER values reported here align well with the theoretical background.

### 3.7. Limitations of the study and outlook

The complexity of the events, evidenced by the different and complex shapes of TSS-discharge hysteresis curves and the lack of complete representation of sampled anticlockwise hysteresis events, may indicate that a higher sampling frequency during events, a higher number of different events, even with lower discharge thresholds for starting the sampling, may be needed to further deepen the understanding of the dynamics of different types of events. Regarding the relation between

soil, sediment and SPM, a higher number of samples from soil and sediment on the one hand and less aggregation into composite samples might be needed to successfully establish a relation between sediment sources and SPM quality. Furthermore, a separation of the solids into different particle size classes could improve the direct comparability of the samples from SPM, soil and sediment, without the need to rely on correction methods like the normalization with Al.

The much higher total element concentrations during event flow compared to low-flow periods is well known and has strong implications for the design of monitoring programs: To be able to quantitatively assess the transport of PTEs, it is necessary to sample during high-flow events, otherwise only a very small share of the metal transport might be observed, which is a problem e.g. for the validation of emission and water quality models at the catchment scale (Fuchs et al., 2017). In small catchments such as those studied here, it is very difficult, if not impossible in practice to carry out such sampling of events without automated samplers triggered by in-line measurements, as the duration of the discharge events is rather short and the TSS peaks are even shorter. The approach applied here of starting the sampling program with a water level trigger and then performing time proportional sampling may not be optimal to properly sample peak concentrations, but it works reliably. Direct triggering of sampling by the turbidity probe was not possible because the turbidity signal showed many artefacts that make it difficult to derive a clean and suitable signal directly during events. Further research is needed to optimise sensor placement, signal processing and signal use for triggering sampling to further improve sampling for this purpose.

## 4. Conclusions

With our study in three different sub-catchments of a lowland river, we were able to show that PTE transport during discharge events is not only driven by the amount of SPM transported, but that the quality of the SPM also changes during events. Higher content of traffic related elements (e.g. Sb) in the earlier stages of events indicate inputs from street runoff and suggest that retention of street runoff in sewers or retention basins could be effectively used to reduce emissions into rivers. The changing quality of SPM has also implications for monitoring of PTE during events. As the quality of SPM varies during the events, the sampling of all stages of the event is necessary for a proper event characterisation or load estimation. The sampled events show mostly complex hysteresis patterns and a higher sampling frequency with a higher number of analysed samples seems necessary to gain further insights into event dynamics.

The investigation of the dissolved share of the PTE concentrations showed a low to moderate pollution level with no exceedance of environmental quality standards in the studied catchment.

The dissolved concentrations, while not as variable as the total concentrations, show significant differences between some events and thus offer high potential to discriminate between different event types. Using the dissolved element concentrations, we were able to identify the duration of pre-event low-flow period as a factor explaining the differences between such events. It was not possible to differentiate between events for total or SPM concentrations after excluding the influence of discharge and TSS concentration level, as the high variability of these factors might overwrite small remaining variability in concentrations. The observed different types of events, at least with regard to the dissolved concentrations, indicate that in each catchment multiple events must be sampled to cover the full variability of event types. Further research is needed to classify events into different categories and to identify further variables that influence PTE concentrations during different events.

The calculation of enrichment factors in combination with local soils as a reference material allowed us to identify which elements are affected by anthropogenic emissions and thus provides some strong indications of important pollution sources and pathways. Enrichment factors were especially high for Ag, Bi, Zn, Cu, P in the catchment with the highest population density and share of treated wastewater in the river runoff. However, with the available samples and analysed elements, it was not possible to successfully implement a fingerprinting approach for the suspended sediments. As added value for emission modelling on the catchment scale, we derived some new and updated enrichment ratios for further use in soil erosion emission modelling.

## Funding

The research has been supported by the Danube Hazard $m^3c$ project (DTP3-299-2.1), co-funded by European Union funds (ERDF, IPA, ENI) and National Funds of the participating countries in the frame of the Interreg Danube Transnational Programme.

## CRediT authorship contribution statement

**Steffen Kittlaus:** Writing – review & editing, Writing – original draft, Visualization, Software, Resources, Methodology, Investigation, Formal analysis, Data curation, Conceptualization. **Radmila Milačič Ščančar:** Writing – review & editing, Validation, Resources, Methodology, Investigation. **Katarina Kozlica:** Writing – review & editing, Validation, Investigation. **Nikolaus Weber:** Writing – review & editing, Validation, Investigation, Data curation. **Jörg Krampe:** Writing – review & editing, Resources. **Matthias Zessner:** Writing – review & editing, Supervision, Funding acquisition, Conceptualization. **Ottavia Zoboli:** Writing – review & editing, Supervision, Project administration, Funding acquisition, Conceptualization.

## Declaration of competing interest

The authors declare that they have no conflicting interests.

## Data availability

The dataset is available under the following DOI: https://dx.doi.org/10.48436/gdt30-hnj49

## Acknowledgements

The authors acknowledge TU Wien Bibliothek for financial support through its Open Access Funding Programme.

## Supplementary material

Supplementary material to this article can be found online at https://doi.org/10.1016/j.jconhyd.2025.104659.

## References

Abwasserverband Eisenstadt-Eisbachtal, 2025. Kläranlage (waste water treatment plant): Wie funktioniert die Kläranlage? (how does the WWTP work?). Schaubild der Kläranlage in Eisenstadt (Diagram of the wastewater treatment plant in Eisenstadt). https://www.awv-eisenstadt.at/klaeranlage (accessed 20 June 2025).

Acosta Porras, E.A., Kishi, R.T., Fuchs, S., Hilgert, S., 2016. Estimation of phosphorus emissions in the upper iguazu basin (Brazil) using gis and the more model. Int. Arch. Photogramm. Remote Sens. Spatial Inf. Sci. XLI-B8, 299–304. https://doi.org/10.5194/isprsarchives-XLI-B8-299-2016.

Aksoy, H., Kavvas, M.L., 2005. A review of hillslope and watershed scale erosion and sediment transport models. Catena 64, 247–271. https://doi.org/10.1016/j.catena.2005.08.008.

Amann, A., Clara, M., Gabriel, O., Hochedlinger, G., Humer, M., Humer, F., Kittlaus, S., Kulcsar, S., Scheffknecht, C., Trautvetter, H., Zessner, M., Zoboli, O., 2019. STOBIMO Spurenstoffe: Stoffbilanzmodellierung für Spurenstoffe auf Einzugsgebietsebene. Wien, p. 371.

Anderson, M.J., 2014. Permutational multivariate analysis of variance (PERMANOVA). In: Balakrishnan, N., Colton, T., Everitt, B., Piegorsch, W., Ruggeri, F., Teugels, J.L. (Eds.), Wiley StatsRef: Statistics Reference Online, 48. Wiley, pp. 1–15.

Auerswald, K., Haider, J., 1992. Eintrag von Agrochemikalien in Oberflächengewässer durch Bodenerosion: Input of agrochemicals into surface waters by soil erosion. Zeitschrift für Kulturtechnik und Landentwicklung 33, 222–229.

Barber, L.B., Paschke, S.S., Battaglin, W.A., Douville, C., Fitzgerald, K.C., Keefe, S.H., Roth, D.A., Vajda, A.M., 2017. Effects of an extreme flood on trace elements in river water-from urban stream to major river basin. Environ. Sci. Technol. 51, 10344–10356. https://doi.org/10.1021/acs.est.7b01767.

Barrett, T., Dowle, M., Srinivasan, A., 2023. data.table: Extension of 'data.frame'. https://CRAN.R-project.org/package=data.table.

Birch, G.F., Matthai, C., Fazeli, M.S., 2006. Efficiency of a retention/detention basin to removecontaminants from urban stormwater. Urban Water J. 3, 69–77. https://doi.org/10.1080/15730620600855894.

Cederkvist, K., Jensen, M., Ingvertsen, S., Holm, P., 2016. Controlling stormwater quality with filter soil—event and dry weather testing. Water 8, 349. https://doi.org/10.3390/w8080349.

Cesco, S., Pii, Y., Borruso, L., Orzes, G., Lugli, P., Mazzetto, F., Genova, G., Signorini, M., Brunetto, G., Terzano, R., Vigani, G., Mimmo, T., 2021. A smart and sustainable future for viticulture is rooted in soil: how to face Cu toxicity. Appl. Sci. 11, 907. https://doi.org/10.3390/app11030907.

Chen, J.-B., Gaillardet, J., Bouchez, J., Louvat, P., Wang, Y.-N., 2014. Anthropophile elements in river sediments: overview from the Seine River, France. Geochem. Geophys. Geosyst. 15, 4526–4546. https://doi.org/10.1002/2014GC005516.

Ciszewski, D., Grygar, T.M., 2016. A review of flood-related storage and remobilization of heavy metal pollutants in river systems. Water Air Soil Pollut. 227, 239. https://doi.org/10.1007/s11270-016-2934-8.

Deutsches Institut für Normung e.V, German standard methods for the examination of water, waste water and sludge; parameters characterizing effects and substances (group H); determination of filterable matter and the residue on ignition (*H2*), DIN 38409-2:1987-03: Deutsche Einheitsverfahren zur Wasser-, Abwasser- und Schlammuntersuchung; Summarische Wirkungs- und Stoffkenngrößen (Gruppe_H); Bestimmung der abfiltrierbaren Stoffe und des Glührückstandes (H 2), 1987. DIN Media GmbH, Berlin. https://doi.org/10.31030/2052931.

Deutsches Institut für Normung e.V, 1998. Water quality - Determination of nitrogen - Part 1: Method using oxidative digestion with peroxodisulfate (ISO 11905-1:1997); German version EN ISO 11905-1:1998: DIN EN ISO 11905-1:1998–08, Wasserbeschaffenheit - Bestimmung von Stickstoff - Teil 1: Bestimmung von Stickstoff nach oxidativem Aufschluß mit Peroxodisulfat (ISO_11905–1:1997). DIN Media GmbH, Berlin. https://doi.org/10.31030/7528261.

Deutsches Institut für Normung e.V, 2004. Water quality - Determination of phosphorus - Ammonium molybdate spectrometric method (ISO 6878:2004); German version EN ISO 6878:2004: DIN EN ISO 6878:2004–09, Wasserbeschaffenheit_- Bestimmung von Phosphor_- Photometrisches Verfahren mittels Ammoniummolybdat (ISO_6878: 2004), 2004th ed. DIN Media GmbH, Berlin. https://doi.org/10.31030/9552789.

Durjava, M.K., Kolar, B., Balk, F., Peijnenburg, W., 2013. Water Framework Directive and specific pollutants in surface waters in Slovenia: Vodna direktiva in posebna onesnaževala za površinske vode v Sloveniji. Acta Hydrotechnica 26.

Durrieu, G., Layglon, N., D'Onofrio, S., Oursel, B., Omanović, D., Garnier, C., Mounier, S., 2023. Extreme hydrological regimes of a small urban river: impact on trace element partitioning, enrichment and fluxes. Environ. Monit. Assess. 195, 1092. https://doi.org/10.1007/s10661-023-11622-x.

EMREG, 2024. Wasserinformationssystem Austria - Emissionsregister (EMREG-OW). Bundesministerium für Land- und Forstwirtschaft, Regionen und Wasserwirtschaft.

European Environment Agency, EU-DEM (raster): version 1.1. 25 m resolution. https://www.eea.europa.eu/en/datahub/datahubitem-view/d08852bc-7b5f-4835-a776-08362e2fbf4b#tab-metadata (accessed 30 October 2024), 2016.

European Environment Agency, 2020b. Imperviousness density 2018 (raster 10 m), Europe, 3-yearly. https://dx.doi.org/10.2909/3bf542bd-eebd-4d73-b53c-a0243f2ed862.

European Environment Agency, 2020a. CORINE land cover 2018: (vector), Europe, 6-yearly - version 2020_20u1, may 2020. https://doi.org/10.2909/71c95a07-e296-44fc-b22b-415f42acfdf0.

European Parliament and the Council of the European Union, 2013. Directive 2013/39/EU of the European Parliament and of the Council of 12 August 2013 amending Directives 2000/60/EC and 2008/105/EC as regards priority substances in the field of water policy: 2013/39/EU.

EUROSTAT - Gisco, Population density grid for Europe 2021: 1 km resolution. https://ec.europa.eu/eurostat/web/gisco/geodata/grids (accessed 4 November 2024), 2023. CC-BY 4.0.

Fuchs, S., Schwarz, M., 2007. Ableitung naturraumtypischer Anreicherungsfaktoren zur Bestimmung des Phosphor-und Schwermetalleintrags in Oberflächengewässer durch Erosion, 1st ed. Karlsruhe.

Fuchs, S., Kaiser, M., Kiemle, L., Kittlaus, S., Rothvoß, S., Toshovski, S., Wagner, A., Wander, R., Weber, T., Ziegler, S., 2017. Modeling of regionalized emissions (MoRE) into water bodies: an open-source river basin management system. Water 9, 239. https://doi.org/10.3390/w9040239.

Gomez Cortes, L., Marinov, D., Sanseverino, I., Navarro Cuenca, A., Niegowska, M., Porcel Rodriguez, E., Stefanelli, F., Lettieri, T., 2022. Selection of Substances for the 4th Watch List under the Water Framework Directive. Publications Office of the European Union, Luxembourg (online resource). ISBN 978-92-76-55020-4.

Hammer, U.T., 1986. Saline Lake Ecosystems of the World. Dr. W. Junk Publishers, Dordrecht.

Haslinger, K., Bartsch, A., 2016. Creating long-term gridded fields of reference evapotranspiration in alpine terrain based on a recalibrated Hargreaves method. Hydrol. Earth Syst. Sci. 20, 1211–1223. https://doi.org/10.5194/hess-20-1211-2016.

Hayes, M.J., 2005. Drought indices. In: Considine, G.D. (Ed.), Van Nostrand's Scientific Encyclopedia. Wiley.

Helsel, D.R., 2011. Statistics for Censored Environmental Data Using Minitab® and R, 2nd ed. John Wiley & Sons, Inc, Hoboken, NJ, USA, p. 324.

Hiebl, J., Frei, C., 2016. Daily temperature grids for Austria since 1961—concept, creation and applicability. Theor. Appl. Climatol. 124, 161–178. https://doi.org/10.1007/s00704-015-1411-4.

Hiebl, J., Frei, C., 2018. Daily precipitation grids for Austria since 1961—development and evaluation of a spatial dataset for hydroclimatic monitoring and modelling. Theor. Appl. Climatol. 132, 327–345. https://doi.org/10.1007/s00704-017-2093-x.

Hydrographischer Dienst Burgenland, 2022. Wasserprotal Burgenland. https://wasser.bgld.gv.at/hydrographie/die-fluesse.

Jiang, J., Li, J., Wang, Z., Wu, X., Lai, C., Chen, X., 2022. Effects of different cropping systems on ammonia nitrogen load in a typical agricultural watershed of South China. J. Contam. Hydrol. 246, 103963. https://doi.org/10.1016/j.jconhyd.2022.103963.

Julian, P., Helsel, D., 2023. NADA2: Data Analysis For Censored Environmental Data. https://CRAN.R-project.org/package=NADA2.

Kardos, M.K., Clement, A., Jolánkai, Z., Zessner, M., Kittlaus, S., Weber, N., Gabriel, O., Broer, M.B., Soare, F., Hamchevici, C., Sidau, M., Tonev, R., Milačič, R., Ščančar, J., Horvat, M., Marković, K., Kulcsar, S., Schuhmann, A., Bordós, G., Pataj, E., Zoboli, O., 2024. Development and testing of an efficient micropollutant monitoring strategy across a large watershed. Sci. Total Environ. 174760. https://doi.org/10.1016/j.scitotenv.2024.174760.

Lee, L., 2020. NADA: Nondetects and Data Analysis for Environmental Data. https://CRAN.R-project.org/package=NADA.

Li, Y., Zhou, Q., Ren, B., Luo, J., Yuan, J., Ding, X., Bian, H., Yao, X., 2020. Trends and health risks of dissolved heavy metal pollution in Global River and Lake water from 1970 to 2017. In: de Voogt, Pim (Ed.), Reviews of Environmental Contamination and Toxicology, vol. 251. Springer, pp. 1–24.

Lloyd, C.E.M., Freer, J.E., Johnes, P.J., Collins, A.L., 2016. Technical note: testing an improved index for analysing storm discharge–concentration hysteresis. Hydrol. Earth Syst. Sci. 20, 625–632. https://doi.org/10.5194/hess-20-625-2016.

Matsunaga, T., Tsuduki, K., Yanase, N., Kritsananuwat, R., Ueno, T., Hanzawa, Y., Naganawa, H., 2014. Temporal variations in metal enrichment in suspended particulate matter during rainfall events in a rural stream. Limnology 15, 13–25. https://doi.org/10.1007/s10201-013-0409-9.

Milačič, R., Zuliani, T., Vidmar, J., Oprčkal, P., Ščančar, J., 2017. Potentially toxic elements in water and sediments of the Sava River under extreme flow events. Sci. Total Environ. 605-606, 894–905. https://doi.org/10.1016/j.scitotenv.2017.06.260.

Milačič, R., Marković, K., Marković, S., Ščančar, J., Jolánkai, Z., Clement, A., Musa, I., Kardos, M.K., Zoboli, O., Zessner, M., 2023. Changes in concentrations of potentially toxic elements during storage of hard river water samples at low temperatures using different sample preservation procedures. J. Soil. Sediment. 23, 4173–4186. https://doi.org/10.1007/s11368-023-03625-5.

Nasrabadi, T., Ruegner, H., Sirdari, Z.Z., Schwientek, M., Grathwohl, P., 2016. Using total suspended solids (TSS) and turbidity as proxies for evaluation of metal transport in river water. Appl. Geochem. 68, 1–9. https://doi.org/10.1016/j.apgeochem.2016.03.003.

Nasrabadi, T., Ruegner, H., Schwientek, M., Bennett, J., Fazel Valipour, S., Grathwohl, P., 2018. Bulk metal concentrations versus total suspended solids in rivers: time-invariant & catchment-specific relationships. PloS One 13, e0191314. https://doi.org/10.1371/journal.pone.0191314.

Oksanen, J., Simpson, G.L., Blanchet, F.G., Kindt, R., Legendre, P., Minchin, P.R., O'Hara, R.B., Solymos, P., Stevens, M.H.H., Szoecs, E., Wagner, H., Barbour, M., Bedward, M., Bolker, B., Borcard, D., Carvalho, G., Chirico, M., Caceres, M.D., Durand, S., Evangelista, H.B.A., FitzJohn, R., Friendly, M., Furneaux, B., Hannigan, G., Hill, M.O., Lahti, L., McGlinn, D., Ouellette, M.-H., Cunha, E.R., Smith, T., Stier, A., Braak, C.J.F.T., Weedon, J., 2024. vegan: Community Ecology Package. https://CRAN.R-project.org/package=vegan.

Oursel, B., Garnier, C., Zebracki, M., Durrieu, G., Pairaud, I., Omanović, D., Cossa, D., Lucas, Y., 2014. Flood inputs in a Mediterranean coastal zone impacted by a large urban area: dynamic and fate of trace metals. Mar. Chem. 167, 44–56. https://doi.org/10.1016/j.marchem.2014.08.005.

Palleiro, L., Rodríguez-Blanco, M.L., Taboada-Castro, M.M., Taboada-Castro, M.T., 2012. Dissolved and particulate metals in the Mero River (NW Spain): factors affecting concentrations and load during runoff events. Commun. Soil Sci. Plant Anal. 43, 88–94. https://doi.org/10.1080/00103624.2011.638528.

Philippe, M., Le Pape, P., Resongles, E., Landrot, G., Freydier, R., Bordier, L., Baptiste, B., Delbes, L., Baya, C., Casiot, C., Ayrault, S., 2023. Fate of antimony contamination generated by road traffic - a focus on Sb geochemistry and speciation in stormwater ponds. Chemosphere 313, 137368. https://doi.org/10.1016/j.chemosphere.2022.137368.

Pourret, O., Hursthouse, A., 2019. It's time to replace the term "heavy metals" with "potentially toxic elements" when reporting environmental research. Int. J. Environ. Res. Public Health 16. https://doi.org/10.3390/ijerph16224446.

Pulley, S., Foster, I., Antunes, P., 2016. The dynamics of sediment-associated contaminants over a transition from drought to multiple flood events in a lowland UK catchment. Hydrol. Process. 30, 704–719. https://doi.org/10.1002/hyp.10616.

Quinton, J.N., Catt, J.A., 2007. Enrichment of heavy metals in sediment resulting from soil Erosion on agricultural fields. Environ. Sci. Technol. 41, 3495–3500. https://doi.org/10.1021/es062147h.

R. Core Team, 2023. R: A Language and Environment for Statistical Computing. R Foundation for Statistical Computing, Vienna, Austria.

Reimann, C., de Caritat, P., 2000. Intrinsic flaws of element enrichment factors (EFs) in environmental geochemistry. Environ. Sci. Technol. 34, 5084–5091. https://doi.org/10.1021/es001339o.

Roussiez, V., Probst, A., Probst, J.-L., 2013. Significance of floods in metal dynamics and export in a small agricultural catchment. J. Hydrol. 499, 71–81. https://doi.org/10.1016/j.jhydrol.2013.06.013.

Saravanan, P., Saravanan, V., Rajeshkannan, R., Arnica, G., Rajasimman, M., Baskar, G., Pugazhendhi, A., 2024. Comprehensive review on toxic heavy metals in the aquatic system: sources, identification, treatment strategies, and health risk assessment. Environ. Res. 258, 119440. https://doi.org/10.1016/j.envres.2024.119440.

Sharpley, A.N., 1985. The selective Erosion of plant nutrients in runoff. Soil Sci. Soc. Am. J. 49, 1527–1534. https://doi.org/10.2136/sssaj1985.03615995004900060039x.

Slowikowski, K., 2024. Ggrepel: Automatically Position Non-Overlapping Text Labels with 'ggplot2'. https://CRAN.R-project.org/package=ggrepel.

Soja, G., Züger, J., Knoflacher, M., Kinner, P., Soja, A.-M., 2013. Climate impacts on water balance of a shallow steppe lake in eastern Austria (Lake Neusiedl). J. Hydrol. 480, 115–124. https://doi.org/10.1016/j.jhydrol.2012.12.013.

Taylor, M., Kruger, N., 2020. Tyre weights an overlooked diffuse source of lead and antimony to road runoff. Sustainability 12, 6790. https://doi.org/10.3390/su12176790.

Taylor, S.R., McLennan, S.M., 1995. The geochemical evolution of the continental crust. Rev. Geophys. 33, 241–265.

Vaiopoulou, E., Gikas, P., 2020. Regulations for chromium emissions to the aquatic environment in Europe and elsewhere. Chemosphere 254, 126876. https://doi.org/10.1016/j.chemosphere.2020.126876.

Venohr, M., Hirt, U., Hofmann, J., Opitz, D., Gericke, A., Wetzig, A., Natho, S., Neumann, F., Hürdler, J., Matranga, M., Mahnkopf, J., Gadegast, M., Behrendt, H., 2011. Modelling of nutrient emissions in river systems - MONERIS - methods and background. Int. Rev. Hydrobiol. 96, 435–483. https://doi.org/10.1002/iroh.201111331.

Viers, J., Dupré, B., Gaillardet, J., 2009. Chemical composition of suspended sediments in world Rivers: new insights from a new database. Sci. Total Environ. 407, 853–868. https://doi.org/10.1016/j.scitotenv.2008.09.053.

Weber, N., Kittlaus, S., Milačič, R., Zessner, M., Krampe, J., Zoboli, O., 2025. The Importance of Eventflow Sampling for River Load Calculation of Micropollutants: Manuscript in Preparation.

Wickham, H., 2016. ggplot2: Elegant Graphics for Data Analysis. Springer-Verlag, New York.

Williams, G.P., 1989. Sediment concentration versus water discharge during single hydrologic events in rivers. J. Hydrol. 111, 89–106. https://doi.org/10.1016/0022-1694(89)90254-0.

Zessner, M., Zoboli, O., Reif, D., Amann, A., Sigmund, E., Kum, G., Saracevic, Z., Saracevic, E., Kittlaus, S., Krampe, J., Wolfram, G., 2019. Belastung des Neusiedler Sees mit anthropogenen Spurenstoffen: Überlegungen zu Herkunft und Verhalten. Österreichische Wasser- und Abfallwirtschaft 71, 522–536. https://doi.org/10.1007/s00506-019-00623-1.

Zhang, X., Barceló, D., Clougherty, R.J., Gao, B., Harms, H., Tefsen, B., Vithanage, M., Wang, H., Wang, Z., Wells, M., 2022. "potentially toxic element"—something that means everything means nothing. Environ. Sci. Technol. 56, 11922–11925. https://doi.org/10.1021/acs.est.2c03056.

Zhuang, W., Song, J., 2021. Thallium in aquatic environments and the factors controlling Tl behavior. Environ. Sci. Pollut. Res. 28, 35472–35487. https://doi.org/10.1007/s11356-021-14388-2.

Zoboli, O., Hainz, R., Riedler, P., Kum, G., Sigmund, E., Hintermaier, S., Saracevic, E., Krampe, J., Zessner, M., Wolfram, G., 2023. Fate of nutrients and trace contaminants in a large shallow soda lake. Spatial gradients and underlying processes from the tributary river to the reed belt. Environ Sci Process Impacts 25, 1505–1518. https://doi.org/10.1039/d3em00152k.